NAVAL POSTGRADUATE SCHOOL
Monterey, California

THESIS

REFRACTIVE TURBULENCE PROFILING
VIA BINARY SOURCE INTENSITY
SCINTILLATION CORRELATION

by

Ricky R. Holland

September 1988

Thesis Advisor: Donald L. Walters

Unclassified

Security Classification of this page

REPORT DOCUMENTATION PAGE

1a Report Security Classification: Unclassified		1b Restrictive Markings	
2a Security Classification Authority		3 Distribution/Availability of Report: Approved for public release; distribution is unlimited.	
2b Declassification/Downgrading Schedule			
4 Performing Organization Report Number(s)		5 Monitoring Organization Report Number(s)	
6a Name of Performing Organization: Naval Postgraduate School	6b Office Symbol (*If Applicable*): 61	7a Name of Monitoring Organization	
6c Address (*city, state, and ZIP code*): Monterey, CA 93943-5000		7b Address (*city, state, and ZIP code*)	
8a Name of Funding/Sponsoring Organization	8b Office Symbol (*If Applicable*)	9 Procurement Instrument Identification Number	
8c Address (*city, state, and ZIP code*)		10 Source of Funding Numbers	
		Program Element Number / Project No / Task No / Work Unit Accession No	

11 Title (*Include Security Classification*): REFRACTIVE TURBULENCE PROFILING VIA BINARY SOURCE INTENSITY SCINTILLATION CORRELATION

12 Personal Author(s): Ricky R. Holland

13a Type of Report	13b Time Covered	14 Date of Report (*year, month,day*)	15 Page Count
Master's Thesis	From To	1988 September	73

16 Supplementary Notation: The views expressed in this thesis are those of the author and do not reflect the official policy or position of the Department of Defense or the U.S. Government.

17 Cosati Codes			18 Subject Terms (*continue on reverse if necessary and identify by block number*)
Field	Group	Subgroup	Refractive Turbulence Profiles, Stellar Scintillation, Photon Counting Statistics

19 Abstract (*continue on reverse if necessary and identify by block number*)

This study examines the binary source correlation technique for determining vertical profiles of the refractive index structure parameter, C_n^2. Theoretical intensity scintillation covariance functions and power spectra for atmospheric layers of depth Δh at a mean altitude of h are derived. These functions are related to the photoelectron counting statistics and the spatial covariance of photoelectron counts for binary point sources. A linear detector array in the exit pupil of an optical system is examined, and the effects of the detection process uncertainty are explored. A lower bound for the expected error of an experimental determination of the spatioangular covariance of counts is derived. This error is then minimized via at least squares analysis using the redundant information available in pairwise multiple correlations of a signal from the detector elements of a ten element linear array. The refractive index structure parameter profile is then derived and found to be the undetermined coefficients of the spatial covariance weighting functions in the least squares analysis.

20 Distribution/Availability of Abstract	21 Abstract Security Classification	
[X] unclassified/unlimited [ ] same as report [ ] DTIC users	Unclassified	
22a Name of Responsible Individual: D.L. Walters	22b Telephone (*Include Area code*): (408) 646-2267	22c Office Symbol: Code 61We

DD FORM 1473, 84 MAR 83 APR edition may be used until exhausted security classification of this page

All other editions are obsolete Unclassified

Approved for public release; distribution is unlimited.

Refractive Turbulence Profiles via Binary Source Intensity Scintillation Correlations

by

Ricky R. Holland
Lieutenant, United States Navy Reserve
B.A., University of Florida, 1981

Submitted in partial fulfillment of the
requirements for the degree of

MASTER OF SCIENCE IN PHYSICS

from the

NAVAL POSTGRADUATE SCHOOL

September 1988

ABSTRACT

This study examines the binary source correlation technique for determining vertical profiles of the refractive index structure parameter, C_n^2. Theoretical intensity scintillation covariance functions and power spectra for atmospheric layers of depth Δh at a mean altitude of h are derived. These functions are related to the photoelectron counting statistics and the spatial covariance of photoelectron counts for binary point sources. A linear detector array in the exit pupil of an optical system is examined, and the effects of the detection process uncertainty are explored. A lower bound for the expected error of an experimental determination of the spatioangular covariance of counts is derived. This error is then minimized via a least squares analysis using the redundant information available in pairwise multiple correlations of a signal from the detector elements of a ten element linear array. The refractive index structure parameter profile is then derived and found to be the undetermined coefficients of the spatial covariance weighting functions in the least squares analysis.

TABLE OF CONTENTS

LIST OF FIGURES

I. INTRODUCTION

The optical remote sensing of refractivity fluctuations induced by turbulent mixing is of the utmost importance to studies of coherent electromagnetic (EM) radiation propagation in the atmosphere. A quantitative characterization of atmospherically induced refractivity fluctuations as a function of altitude is required in the design and system analysis of adaptive optical systems.

Adaptive optical systems are systems that attempt to correct a perturbed wavefront via mechanical or electrooptic methods. These methods include systems with mechanically deformable optical surfaces and phase conjugation techniques using nonlinear optical materials. However, the implementation of these techniques to correct for atmospheric degradation of optical signal quality depends on a thorough probe of atmospheric optical effects.

Typically, three quantities are used to characterize the atmospheric propagation. These are the isoplanatic angle (θ_0), the spatial coherence length of the atmosphere (r_0) and vertical profiles of the refractive index structure parameter C_n^2. The purpose of this thesis is to study theoretically a single technique, binary source correlation, with the intent of finding a robust optical technique to profile the refractive index structure parameter.

Several different approaches to the profiling problem have been employed with varying degrees of success. These include both active and passive means. Active probes of atmospheric structure include acoustic

sounders (up to approximately 1 km) [Refs. 1,2] and pulsed Doppler radar (3-20 km) [Refs. 3,4]. Also, direct profile measurements may be made using microthermal probes mounted on a balloon [Ref. 5]. Passive means of finding the propagation path variations of the structure parameter include direct inversion of the amplitude scintillation covariance function [Refs. 6,7], spatially filtered apertures [Refs. 8,9] and the crossed beam or binary source technique.

The crossed beam method was originally proposed by Fisher and Krause [Ref. 10] and also by Wang, Clifford and Ochs [Ref. 11]. Essentially, the crossed beam technique proposed that two optical sources and two receivers be arranged such that the beams from the sources cross at a point in space. The cross correlation of the receiver outputs allow the determination of the turbulence characteristics at the beam crossing point. The crossed beam technique, hereafter known as the binary source method, was implemented experimentally by several French teams [Refs. 12-15] using a binary star for the source. This method had advantages not present in the aforementioned passive techniques.

The greatest advantages of the binary source technique are high spatial resolution and numerical stability of the algorithm. This is in sharp contrast with techniques involving the inversion of an integrated profile. The inversion of the scintillation covariance is often unstable due to noise [Ref. 16]; and, the spatial filtering technique has limited spatial resolution due to the width of the altitude weighting functions [Refs. 8,9]. Additionally, an artificial source will be available on the relay mirror experiment satellite and it is hoped that these techniques will be directly applicable to profile determinations made using time delayed correlations from this source. [Ref. 17]

II. THEORETICAL BACKGROUND

To fully appreciate the binary source method requires an understanding of the theory of EM propagation in turbulent media. The seminal work in this field was carried out in the Soviet Union in the 1940s and 1950s and this work is summarized in Tatarski [Ref. 18]. Modern treatments of the propagation problem in terms of the formalism of scattering theory have yielded a better understanding of the propagation problem; however, this formalism has proven impotent in furthering the predictive power of the classical theory [Ref. 19].

The classical theory as developed by Tatarski and also summarized by Clifford [Ref. 19], relies on a statistical description of the properties of the turbulent medium. A summary of these properties follows.

A. TURBULENCE IN GENERAL

Turbulence is a property of fluid flows and these flows are governed by the Navier-Stokes equations. The flow is usually characterized by a dimensionless parameter called the Reynolds number, Re, with

$$Re = vL/\mu. \tag{2.1}$$

The quantities v,L and μ are the characteristic velocity, length scale and kinematic viscosity respectively. For small values of Re viscous dissipation dominates and the flow is laminar. As Re grows in magnitude, then a critical value is reached (approximately 1000 in the atmosphere) beyond which fluctuations in the velocity field are no longer damped. For values of Re greater than Re critical the flow rapidly becomes chaotic.

Following Lumely [Ref. 20], there are several distinguishing characteristics of turbulent flow. These are:

- irregularity
- large Reynolds numbers
- diffusivity
- dissipation
- three dimensional vorticity fluctuations.

The characteristics listed above are essential elements of any turbulent flow. For example, the diffusivity of velocity fluctuations in a turbulent flow and the rapid mixing inherent in this process causes an increase in the rates of momentum and heat transfer.

Turbulence is also characterized by three dimensional fluctuations of the vorticity; and, no flow of less than three dimensions is truly considered turbulent. The vorticity fluctuations take place at multiple spatial scales with each scale characterized by a different value of Re.

The energy in a turbulent flow is ultimately dissipated by viscous friction. This dissipation converts the macroscopic kinematic energy of the flow to thermal energy; and, this occurs at the smallest or inner scale of turbulence. Fluctuations with a scale dimension less than the inner scale (1-10 mm in the atmosphere) are damped by viscous dissipation.

The largest scale in a turbulent flow is determined by the boundary conditions. This largest or outer scale of turbulent motion is where energy is pumped into the flow. The energy then cascades from the largest to the smallest scale sizes adiabatically and the energy is dissipated at the inner scale. The range of scales between l_0 and L_0, the inner and outer scales, is called the inertial subrange.

The inertial subrange is so called because the time scale associated with the inertial transfer of energy from larger to smaller scales is much shorter than the time scale characterizing dissipation; therefore, the energy transfer is essentially adiabatic. However, the Reynolds number is dependent on the scale and decreases as the scale decreases. When a scale is reached such that Re is less than the critical value then laminar motion results at that scale size and smaller. Using this fact and the definition of the Reynolds number, the inner and outer scales may be related (within a constant) by dimensional analysis [Ref. 18]. The resulting relationship is

$$(l_o/L_o)^{-4/3} = Re \tag{2.2}$$

with Re the Reynolds number of the flow as a whole.

The existence of a well defined inertial subrange provides a handle by which the statistical analysis of turbulence is carried out. This approach is pursued further in the following sections.

B. STATISTICAL DESCRIPTION OF TURBULENCE

The Navier-Stokes equations are ill-posed since there are more variables than equations; and, unsolvable unless certain restrictive assumptions are made. Unfortunately, these same restrictions exclude the turbulent regime of solutions and a statistical approach is required to analyze the flow.

The full statistics would consist of a knowledge of the multidimensional probability distribution for the velocity field. However, the statistical analysis is complicated by the fact that turbulence is a nonstationary process. Nonstationarity implies that the mean and higher order moments of the velocity field are also stochastic functions of time. Currently, the only well

founded statistical analysis of the velocity field statistics is due to Kolmogorov and is valid only for scales in the inertial subrange of fully developed turbulence. [Ref. 18]

Though the ordinary moments of the velocity field distribution are non-stationary, a statistical analysis based on a second order quantity called the structure tensor is carried out by Tatarski [Ref. 18]. The structure tensor is defined in general by:

$$D_{ij}(\underline{r}) = \langle [v_i(\underline{r}_1+\underline{r})-v_i(\underline{r}_1)]\,[v_j(\underline{r}_1+\underline{r})-v_j(\underline{r}_1)] \rangle \quad , \tag{2.3}$$

with the angled brackets representing an ensemble average. This quantity is approximately stationary for scale sizes in the inertial subrange. The structure tensor may be further simplified by three assumptions and these are:

- local homogeneity
- local isotropy
- incompressible turbulence.

Homogeneity implies that the structure tensor depends only on the displacement $\underline{r}$ and not a particular location in space. Isotropy implies rotational invariance or radial symmetry in that only the magnitude of $\underline{r}$ and not the direction is important. The assumption of local homogeneity and isotropy is a weaker assumption that reflects the fact that the structure tensor depends only on scales very close to r. With the third assumption of incompressibility, that is the divergence of $\underline{v}$ equals zero [Ref. 21], homogeneity and isotropy yield the following expression for the structure function:

$$D_{rr}(r) = \langle [v_r(r_1+r)-v_r(r_1)]^2 \rangle \quad , \tag{2.4}$$

where D_{rr} is the projection of the structure tensor in the direction parallel to the displacement $\underline{r}$. This function describes the statistics of homogeneous, isotropic and incompressible turbulence. [Ref. 19]

For values of r in the inertial subrange of scales dimensional analysis of the structure function yields:

$$D_{rr} = C_v^2 r^{2/3} \tag{2.5}$$

with C_v^2 the velocity structure parameter [Ref. 18]. The structure parameter is a measure of the intensity of the turbulence and it is directly related to the refractive index structure constant mentioned in the introduction.

1. Atmospheric Refractivity Fluctuations

To relate the velocity structure function to extensive variables such as the temperature or refractivity then conservative passive additives must be considered [Ref. 18]. Conservative passive additives are those quantities that have no effect on the statistical analysis of the turbulent dynamics; however, the conservative passive additive is transported and mixed by the velocity fluctuations. An example of a conservative passive additive is potential temperature θ, given by:

$$\theta = T(p_o/p)^{.286} \tag{2.6}$$

with T the absolute temperature in Kelvin, p the atmospheric pressure and p_o the pressure at sea level. This quantity is independent of altitude.

Following Clifford [Ref. 19], the potential temperature fluctuation is related to the refractive index fluctuation by:

$$\Delta n = -79 \times 10^{-6}(p/\theta^2)\Delta\theta \tag{2.7}$$

with p the atmospheric pressure in millibars. Since θ is a conservative passive additive then so is the refractivity n. And as shown by Tatarski [Ref. 18], conservative passive additive structure functions obey the same power law as the velocity statistics except near the viscous convective subrange which is near the inner scale. [Ref. 20] Therefore, the structure function for refractive index fluctuations is given by:

$$D_n(r) = C_n^2 r^{2/3}. \tag{2.8}$$

The refractive index structure function is used to find the power spectrum of refractive index fluctuations and since Clifford's derivation [Ref. 19] is clear it is summarized here.

2. Power Spectrum of Refractivity Fluctuations

The refractive index at a point $\underline{r}$ can be decomposed into a mean and a fluctuating part

$$n(\underline{r}) = \langle n(\underline{r}) \rangle + n_1(\underline{r}). \tag{2.9}$$

If n_1 is an analytic function then the spatial frequency spectrum can easily be determined by finding the spatial Fourier transform of $n_1(\underline{r})$. However, since n_1 is a stochastic function then the spatial frequency decomposition is carried out using the three dimensional Fourier-Stieltjes integral

$$n_1(\underline{r}) = \int \exp(i\underline{K} \bullet \underline{r}) dN(\underline{K}) \tag{2.10}$$

Forming the covariance of the refractive index fluctuations,

$$B(\underline{r}+\underline{r}_1, \underline{r}_1) = \langle n_1(\underline{r}+\underline{r}_1) n_1(\underline{r}_1) \rangle \ , \tag{2.11}$$

the power spectrum is found by using the Wiener-Khinchin theorem.

The Wiener-Khinchin theorem asserts that the power spectrum and covariance form a Fourier transform pair. Using this and by invoking homogeneity and isotropy, Clifford [Ref. 19] expresses the power spectrum of refractive index fluctuations as:

$$\Phi_n(K) = \frac{1}{2\pi^2 K}\int_0^\infty drrB_n(r)\sin(Kr) \tag{2.12}$$

This expression is simplified further by use of the following relation between the structure function and the covariance:

$$B_n(0) - B_n(r) = \frac{1}{2} D_n(r) \tag{2.13}$$

Using this relationship and in the limit that the outer scale and inner scale go to infinity and zero respectively the spatial power spectrum becomes:

$$\Phi_n(K) = .033C_n^2K^{-11/3} \tag{2.14}$$

Actually, this expression is valid only for spatial wave numbers such that $2\pi L_o^{-1} << K << 2\pi l_o^{-1}$ with the limiting process used to derive it being only an analytical convenience.

With these expressions in hand the first order theory of optical propagation in the atmosphere is addressed in the next section.

C. FIRST ORDER THEORY OF EM PROPAGATION IN THE ATMOSPHERE

The first order theory of the propagation of an EM wave in the atmosphere is essentially equivalent to first order scattering theory in which the Born approximation allows an approximate solution to the wave equation.

This approach assumes single scattering of a monochromatic wave incident on the atmosphere and it is valid for relatively weak turbulence. For strong turbulence multiple scattering effects cause many of the statistical quantities of interest to saturate to a constant value; however, except for long propagation paths through strong turbulence (1-2 km in the late afternoon) the first order theory proves adequate for many purposes.

The first order theory assumes that the atmosphere has unit magnetic permeability and zero conductivity and that the incident EM wave has a sinusoidal time dependence. With these assumptions both Tatarski and Clifford form the scalar wave equation for the propagation of a component of the electric field. Clifford [Ref. 19] proceeds to solve this equation by the method of smooth and small perturbations and this solution is summarized here.

1. Solution of the Wave Equation

Since the electric field is proportional to the magnetic field, and assuming that depolarization effects are negligible, then Clifford shows that it is necessary to analyze only one component of the full vector wave equation. The equation to be solved is:

$$\nabla^2 E + k^2 n^2 E = 0 \tag{2.15}$$

with E one of the components of the electric field, k the wave number of the radiation and n is the position dependent atmospheric refractive index.

The solution to this equation is found by expanding E in a series of decreasing terms:

$$E = E_0 + E_1 + E_2 + \ldots \tag{2.16}$$

with the zero order term corresponding to the unperturbed field, the first order term the single scattering term and higher order terms corresponding to multiple scattering. Retaining the terms to first order and using equation 2.9 then equation 2.15 is resolved into the two equations:

$$\nabla^2 E_0 + k^2 E_0 = 0 \tag{2.17}$$

$$\nabla^2 E_1 + k^2 E_1 + 2k^2 n_1 E_0 = 0 \tag{2.18}$$

This separation is accomplished by substituting $E = E_0 + E_1$ and equating terms of the same order to zero while neglecting terms of order n_1^2 or higher. At this point it should be noted that each term E_m in the perturbative expansion is assumed to be of order n_1^m. Following Clifford and Tatarski [Ref. 18-19] the unperturbed field is assumed to be a unit amplitude plane wave propagating in the z direction and E_0 becomes:

$$E_0 = \exp(ikz) \quad . \tag{2.19}$$

Substituting this into the source term of equation 2.18 then this equation becomes the nonhomogeneous Helmholtz equation for the perturbed electric field E_1:

$$\nabla^2 E_1 + k^2 E_1 = -2k^2 n_1 e^{ikz} \tag{2.20}$$

The formal solution of this equation is well known and it is the convolution of the source term of equation 2.20 with the Helmholtz equation Green's function:

$$E_1(\underline{r}) = \frac{1}{4\pi} \int d^3\underline{r}' \frac{e^{ik|\underline{r}-\underline{r}'|}}{|\underline{r}-\underline{r}'|} \left[2k^2 n_1(\underline{r}') e^{ikz'} \right] \tag{2.21}$$

with the integration over the scattering volume.

To simplify the formal solution further the Fraunhofer approximation is made in equation 2.21. The Fraunhofer approximation assumes that λ is much less than the size of the scattering refractive index inhomogeneity so that radiation is scattered in a small forward cone. In fact, if the varying refractive index is perceived as a weak phase screen then qualitatively the angle of scattering will be a maximum for inhomogeneities on the order of the inner scale. Therefore, from simple diffraction theory the maximum scattering angle should be on the order of λ/l_0 with λ the wavelength; and, for inner scales on the order of millimeters then this angle is on the order of 10^{-4} radians. Specifically, the Fraunhofer approximation assumes that the vertical distance from scatterer to receiver, $|z-z'|$, is much greater than the transverse displacement, $|\rho-\rho'|$, from the z axis. Making the Fraunhofer approximation means replacing the term $|\underline{r}-\underline{r}'|$ in the denominator of equation 2.21 by $|z-z'|$ and expanding the term $|\underline{r}-\underline{r}'|$ in a binomial series retaining terms to second order in the phase. The resulting expression for the perturbed field E_1 is:

$$E_1(\underline{r}) = \frac{k^2 e^{ikz}}{2\pi} \int_{vol} d^3\underline{r}' \exp\left\{\frac{ik(\rho-\rho')}{2(z-z')}\right\} \frac{n_1(\underline{r}')}{(z-z')} \qquad (2.22)$$

The physical interpretation of this equation is that of a spherical Huygen's wavelet emitted at the scattering weak phase screen. The fringes produced by the interference of the Huygen's wavelet with the unscattered plane wave are interpreted as the amplitude and phase perturbations observed in atmospheric optical propagation.

For the task at hand the quantities of interest are the fluctuations of the amplitude and the intensity of the optical signal about the unperturbed

values. To find the amplitude fluctuations both Tatarski and Clifford use the Rytov approximation which assumes that the solution of the wave equation is of the form

$$E = Ae^{is} \; ; \tag{2.23}$$

with A an amplitude and s a complex phase. Letting $E_o = A_o \exp(is_o)$ then the ratio E/E_o becomes:

$$\frac{E}{E_o} = 1 + \frac{E_1}{E_o} = \frac{A}{A_o} \exp\left[i(S-S_o)\right] \tag{2.24}$$

And, taking the natural log of equation 2.24 splits the ratio into real and imaginary parts as follows:

$$\log\left(1 + \frac{E_1}{E_o}\right) = \log\left(1 + \frac{A_1}{A_o}\right) + i\,(S-S_o) \tag{2.25}$$

Since E_1 is assumed much less than E_o and also that $A_1 << A_o$, then the logarithm can be expanded quite accurately in a Taylor series. Carrying out this expansion and retaining terms to first order yields:

$$\frac{E_1}{E_o} \cong \frac{A_1}{A_o} + i\,(S-S_o) \tag{2.26}$$

Following Clifford this implies that the amplitude ratio is approximately the real part of equation 2.22 normalized by the unperturbed field E_o. This yields the following expression for the amplitude ratio:

$$\frac{A_1}{A_o} = \frac{k^2}{2\pi} \int_{vol} d^3\underline{r}' \cos\left[\frac{k(\rho-\rho')}{2(z-z')}\right] \frac{n_1(\underline{r}')}{(z-z')} \tag{2.27}$$

Tatarski shows that inherent in this approximation is the assumption that the amplitude perturbation is small over the distance of one wavelength of

the radiation. This is called the assumption of smooth perturbations and this condition is virtually always satisfied for optical radiation.

Conventionally, a quantity called the log amplitude is defined such that:

$$x(\underline{r}) = \ln(A/A_0) \approx A_1/A_0 \tag{2.28}$$

Since from the weak scattering viewpoint the log amplitude, $x(\underline{r})$, is equal to the normalized amplitude fluctuation A_1/A_0 then it will be used in all further calculations.

To proceed further the stochastic variable $n_1(\underline{r}')$ in equation 2.27 is expanded in a two-dimensional Fourier-Stieltjes integral:

$$n_1(\underline{r}') = \int d\sigma(\underline{K},z') \exp(i\underline{K}\cdot\underline{\rho}) \tag{2.29}$$

with the expansion in a plane perpendicular to the propagation direction. The random amplitude $d\sigma$ now becomes a function of z', the location along the propagation path. Substituting this expression into equation 2.27 and carrying out the indicated integrations, Clifford obtains the following expression for the log amplitude:

$$x(\underline{r}) = \int e^{i\underline{K}\cdot\underline{\rho}} \left(k \int dz' d\sigma(\underline{K},z') \sin\left[\frac{K^2(z-z')}{2k}\right]\right) \tag{2.30}$$

Using this expression the second order statistics of the observed amplitude fluctuations and the power spectrum of these fluctuations is derived in the next section.

2. Covariance and Power Spectrum of Log Amplitude Fluctuations

The spatial covariance of the log amplitude fluctuations is found by using equation 2.30 and the relation:

$$B_x(\rho,z) = \langle x(\rho_1+\rho,z)\, x^*(\rho_1,z)\rangle \tag{2.31}$$

Following Clifford and inserting equation 2.30 into equation 2.31 the spatial covariance function is written as:

$$B_x(\rho,z) = k^2 \iint e^{i[\underline{K}\cdot(\rho_1+\rho)-\underline{K}'\cdot\rho]} \iint dz'dz'' \sin\left[\frac{K^2(z-z')}{2k}\right]$$

$$\sin\left[\frac{K^2(z-z'')}{2k}\right] \langle d\sigma(\underline{K},z')d\sigma(\underline{K},z'')^*\rangle \tag{2.32}$$

with the superscript * denoting the complex conjugate. The ensemble average of the random complex amplitudes is expressed in terms of the two dimensional spectral density of the refractive index fluctuations, $F_n(\underline{K}', z'-z'')$, by using equation 1.5 in Tatarski [Ref. 18]:

$$\langle d\sigma(\underline{K},z')d\sigma(\underline{K},z'')^*\rangle = \delta(\underline{K}-\underline{K}')F_n(\underline{K}',z'-z'')d^2\underline{K}d^2\underline{K}' \tag{2.33}$$

with $\delta(\underline{K}-\underline{K}')$ a three-dimensional delta function. The two-dimensional spectrum of refractivity fluctuations is defined using the three-dimensional spectrum Φ_n of equation 2.14 and is written as:

$$F_n(\underline{K}',z'-z'') = \int_{-\infty}^{\infty} dK_z \Phi_n(\underline{K}',K_z) \cos\left[K_z(z'-z'')\right] \tag{2.34}$$

Substituting equation 2.33 into equation 2.32, the observed spatial covariance of the log amplitude fluctuations becomes:

$$B_x(\rho,z) = \int d^2\underline{K}\, e^{i[\underline{K}\cdot\rho]} \left\{ k^2 \iint dz'dz'' \sin\left[\frac{K^2(z-z')}{2k}\right] \right.$$

$$\left. \sin\left[\frac{K^2(z-z'')}{2k}\right] F_n(\underline{K},z'-z'') \right\} \tag{2.35}$$

This integral is the Fourier transform of the quantity in the curly brackets. Using the Wiener-Khinchin theorem the expression in the curly brackets is identified with the power spectrum of the log amplitude fluctuations.

To proceed further the experimental geometry as it bears on the evaluation of the integrals for the covariance and power spectrum must be considered. The following sections evaluate the above expressions as they apply directly to the binary source method of structure constant profiling.

III. THE ANALYSIS OF THE EXPERIMENT

The purpose of this calculation is to develop the binary source technique theoretically for application to a linear array of photosensitive or photoemissive detectors in the exit pupil of an optical imaging system. The optical system is assumed to be well corrected with an approximately constant modulation transfer function over the range of spatial wave numbers included in the inertial subrange of turbulence. With this assumption, the intensity distribution in the exit pupil is related to the intensity distribution in the aperture by a simple scaling. Therefore, this calculation examines the experimental geometry illustrated in Figure 1. The exact scaling relations and corrections for a nonideal modulation transfer function will be developed in a later section.

A. GEOMETRICAL CONSIDERATIONS

The binary source technique determines the C_n^2 profile by finding the covariance of scintillations due to a finite number of atmospheric layers Δh. And, a consideration of the geometry of Figure 1 is used to simplify the analysis.

The prototypical binary source of Figure 1 is a binary star with components labeled 1 and 2. Two portions of the wave fronts intercepted by the detector elements are illustrated and the following quantities are defined:

$\underline{d} = \underline{r}_1 - \underline{r}_2$ with $\underline{d}$ the detector element separation from center to center.

Δd, the detector element width.

h, the mean crossing altitude of the wavefronts as illustrated.

Δh, width of crossing.

h_2,h_1; the maximum and minimum altitudes of crossing, respectively.

θ, the angular separation of the binary components 1 and 2.

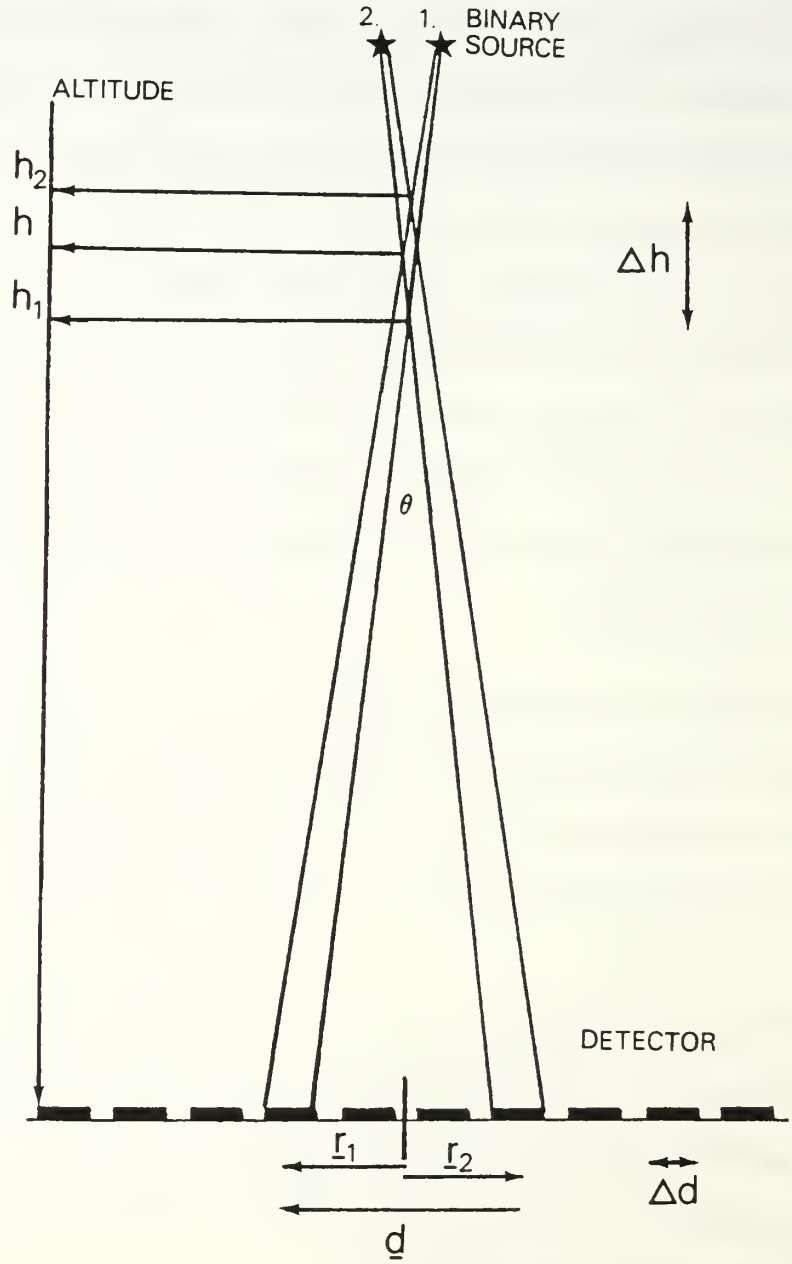

Figure 1. The Experimental Geometry

With these definitions and examining the geometry of Figure 1, two relationships between these variables are apparent:

$$d = \theta h \tag{3.1}$$

$$\Delta d = \theta \Delta h/2 \tag{3.2}$$

Equation 3.1 gives the connection between the detector element separation, d, and the crossing altitude, h. The second equation gives the relation between the detector element width and the width of the crossing at a mean height of h. Equation 3.2 is simply derived by considering the difference between the maximum and minimum crossing altitudes and using equation 3.1. Note that equation 3.1 assumes that the detector array is parallel to a line segment joining the apparent positions of the binary source components. If this condition is not satisfied then equation 3.1 becomes:

$$d = \theta h \sec \phi \tag{3.3}$$

with ϕ the azimuthal angle between the array and the line joining the source components. Equation 3.1 is assumed valid for this calculation; since, the optical system can in principle be aligned and driven such that this relation holds.

B. POWER SPECTRUM OF LOG AMPLITUDE FLUCTUATIONS IN Δh

Given a picture of the experimental geometry the derivation of the power spectrum of log amplitude fluctuations for a layer Δh at an altitude of h is carried out using equation 2.35. This power spectrum is then used to find the expected spatial covariance of the log amplitude fluctuations and the related covariance of intensity scintillations via the Wiener-Khinchin theorem.

For a layer Δh, isotropy and equation 2.35 imply the following expression for the power spectrum of the log amplitude fluctuations:

$$F_x(K,0) = k^2 \int_0^{\Delta h}\int dz'dz'' \sin K^2\frac{(z-z')}{2k}$$

$$\sin \frac{K^2(z-z'')}{2k} F_n(K,z'-z'') \qquad (3.4)$$

with $F_n(K,z'-z'')$ equal to $F_n(K,z''-z')$ the two-dimensional power spectrum of refractive index fluctuations [Ref. 19]. Also note that the origin of the coordinate system is at h_2 (z=0) and the integration is over the scattering volume or layer.

To make full use of the symmetry in equation 3.4 the following variable change is made [Ref. 18]:

$$\xi = z'-z'' \quad \text{and} \quad 2\eta = z'+z'' \qquad (3.5)$$

Using the Jacobian of this transformation then,

$$dz'dz'' = \begin{vmatrix} \partial z'/\partial\xi & \partial z''/\partial\xi \\ \partial z'/\partial\eta & \partial z''/\partial\eta \end{vmatrix} d\xi d\eta = \begin{vmatrix} 1/2 & -1/2 \\ 1 & 1 \end{vmatrix} d\xi d\eta \qquad (3.6)$$

therefore, $dz'dz'' = d\xi d\eta$. Using this variable change and the trigonometric identity $\sin(a+b)\sin(a-b) = \sin^2 a - \sin^2 b$ with,

$$a = \frac{K^2}{2k}(z-\eta)\,; \qquad b = \frac{K^2}{2k}\left(\frac{\xi}{2}\right) \qquad (3.7)$$

then equation 3.4 becomes:

$$F_x(K,0) = k^2 \iint_{\xi\eta} d\xi d\eta F_n(K,\xi)\left[\sin^2\left(\frac{K^2(z-\eta)}{2k}\right) - \sin^2\left(\frac{K^2\xi}{4k}\right)\right] \qquad (3.8)$$

The integrand is simplified further by noting Tatarski's observation on page 135 of Reference 18 that $F_n(K,\xi)$ rapidly approaches zero for $K\xi$ greater than or equal to unity. This derives from the fact that fluctuations in the refractive index separated by displacements greater than L_o, the outer scale, are uncorrelated; and, by the Wiener-Khinchin theorem the power spectrum vanishes as the corresponding covariance of fluctuations goes to zero. Also note that the assumption of smooth perturbations, $\lambda << l_o$, implies that $k >> K$ over the significant part of the integrand of equation 3.8. Therefore, over the significant part of the range of integration then:

$$\frac{K^2\xi}{4k} << 1 \qquad \text{and} \qquad \sin^2\frac{K^2\xi}{4k} \approx 0 \quad . \qquad (3.9)$$

And, equation 3.8 simplifies to:

$$F_x(K,0) = k^2 \iint_{\xi\eta} d\xi d\eta\, F_n(K,\xi) \sin^2\left(\frac{K^2(z-\eta)}{2k}\right) \qquad (3.10)$$

The evaluation of this integral depends on the assumption of a form for $F_n(K,\xi)$ and this form depends on the magnitude of Δh compared with the inner and outer scale. For the experimental geometry of Figure 1 the ten detector elements of the linear array will divide the total atmospheric volume into ten separate non-overlapping regions. The width of these regions will be on the order of kilometers for observations of the profile from the planetary boundary layer to about 20 kilometers. This is much greater than outer scales observed in the atmosphere [Ref. 2,19] and it is safely assumed that $\Delta h >> L_o$.

Under the conditions discussed in the previous paragraph the layer Δh includes many separate, uncorrelated regions of turbulence. Following Tatarski [Ref. 18] the power spectrum of refractive index fluctuations for sublayers of Δh on the order of the outer scale is still given by equation 2.14; however, the refractive index structure constant is now a function of η. Therefore, the refractive index fluctuation power spectrum takes the form:

$$F_n(K,\xi,\eta) = C_n^2(\eta)\, f_n(K,\xi) \tag{3.11}$$

and, it should be noted that:

$$\int f_n(K,\xi)d\xi = \pi(.033)\, K^{-11/3} = \pi\, \Phi_n^o(K) \tag{3.12}$$

with this expression completely analogous to equation 2.14. With an expression for the refractive index power spectrum available further progress in evaluating the integral of equation 3.10 is possible.

Noting that equation 3.10 is even in ξ and symmetric in η then substituting equation 3.11 into equation 3.10 and employing symmetry yields:

$$F_x(K,0) = 2k^2 \int_0^{\Delta h/2} d\eta C_n^2(\eta) \sin^2\left(\frac{K^2(z-\eta)}{2k}\right) \int_0^{2\eta} f_n(K,\xi)d\xi$$
$$+ 2k^2 \int_{\Delta h/2}^{\Delta h} d\eta C_n^2(\eta) \sin^2\left(\frac{K^2(z-\eta)}{2k}\right) \int_0^{2(\Delta h-\eta)} f_n(K,\xi)d\xi \tag{3.13}$$

for the log amplitude power spectrum. Over most of the region of integration both 2η and $2(\Delta h-\eta)$ have magnitudes between the outer scale and Δh. As previously noted, the refractive index power spectrum rapidly

approaches zero for $K\xi$ greater than or equal to one [Ref. 18], therefore the upper limits for the ξ integration are replaced with infinity to a high degree of accuracy. Replacing the upper limits of the ξ integrals of equation 3.13 and carrying out the integrations using equation 3.12 yields the following expression for the power spectrum:

$$F_x(K,0) = 2k^2\pi \int_0^{\Delta h} \Phi_n^0(K) C_n^2(\eta) \sin^2\left[\frac{K^2(z-\eta)}{2k}\right] d\eta \qquad (3.14)$$

Since the detector elements have a finite width then by equation 3.2 spatial variations of C_n^2 smaller than Δh cannot be resolved. In effect the detector observes an average structure constant for the layer. If the C_n^2 profile is known apriori then this average can be carried out in the Fourier transform or spatial covariance domain as an aperture average over the finite detector element area. However, since a measurement of the structure parameter profile is the objective then it is the power spectrum that must be averaged over the layer depth. This average of equation 3.14 is indicated as:

$$\left\langle F_x(K,0) \right\rangle = 2k^2\pi \int_0^{\Delta h} \Phi_n^0(K) \left\langle C_n^2(\eta) \sin^2\left[\frac{K^2(z-\eta)}{2k}\right] \right\rangle d\eta \qquad (3.15)$$

with the angled brackets denoting the spatial average over the layer. The η integration is trivially:

$$\left\langle F_x(K,0) \right\rangle = 2k^2\pi \, \Phi_n^0(K) \Delta h \left\langle C_n^2(\eta) \sin^2\left[\frac{K^2(z-\eta)}{2k}\right] \right\rangle \qquad (3.16)$$

Past observations of C_n^2 indicate that it fluctuates rapidly in space with a mean that decreases slowly with altitude [Refs. 2,19]. Since the spatial fluctuations of C_n^2 appear uncorrelated with the $\sin^2$ weighting function then the average indicated in equation 3.16 is rewritten as:

$$\left\langle F_x(K,0)\right\rangle = 2k^2\pi\,\Phi_n^o(K)\Delta h\left\langle C_n^2(\eta)\right\rangle\left\langle \sin^2\left[\frac{K^2(z-\eta)}{2k}\right]\right\rangle \qquad (3.17)$$

Carrying out the spatial average explicitly for the $\sin^2$ weighting function yields:

$$\left\langle F_x(K,0)\right\rangle = 2k^2\pi\Delta h\Phi_n^o(K)\left\langle C_n^2(\eta)\right\rangle\frac{1}{\Delta h}\int_o^{\Delta h}\sin^2\left[\frac{K^2(z-\eta)}{2k}\right]d\eta \qquad (3.18)$$

or, for z, the observer coordinate, equals h_2:

$$\left\langle F_x(K,0)\right\rangle = 2k^2\pi\,\Delta h\Phi_n^o(K)\left\langle C_n^2(\eta)\right\rangle$$

$$\bullet\left[1-\frac{2k}{\Delta hK^2}\cos\left(\frac{K^2h}{k}\right)\sin\left(\frac{K^2\Delta h}{2k}\right)\right] \qquad (3.19)$$

with $\langle C_n^2(\eta)\rangle$ the average or effective value of the structure parameter for the layer at a mean altitude of h. This is the observed average power spectrum of the log amplitude fluctuations due to turbulent mixing in a layer Δh.

The power spectrum used by the various French teams [Refs. 12-15] is in this calculation's notation written as:

$$F_x(K,0) = 2k^2\pi\Delta h\Phi_n^o(K)\left\langle C_n^2(\eta)\right\rangle\sin^2\left(\frac{K^2h}{2k}\right) \qquad (3.20)$$

Approximating the $\sin(K^2\Delta h/2k)$ term in equation 3.19 by $\Delta hK^2/2k$ ($k >> K$) then 3.19 becomes:

$$\left\langle F_x(K,0)\right\rangle = 2k^2\pi\Delta h\Phi_n^o(K)\left\langle C_n^2(\eta)\right\rangle \sin^2\left(\frac{K^2h}{2k}\right) \qquad (3.21)$$

an expression identical to the French spectrum. The two spectra are illustrated in Figure 2 and it is evident that the French spectrum is an excellent approximation to the spectrum of equation 3.19. Therefore, the spectrum of equation 3.21 will be used for further calculations since it is analytically simpler.

C. THE SPATIOANGULAR CORRELATION OF INTENSITY FLUCTUATIONS

The power spectral density of equation 3.21 can be Fourier transformed to yield the spatial covariance of the log amplitude fluctuations of a single point source due to a layer Δh. The solution of the wave equation in Section II assumed a plane wave solution and as is well known from classical optics a point source at infinity produces plane waves at the detector. For the stellar sources of Figure 1, the transverse spatial coherence function is essentially unity for displacements of less than five meters as shown by Hanbury-Brown and Twiss for Sirius [Ref. 22]. Therefore, an assumption of initial spatial coherence of the source is excellent for spatial separations of less than five meters. However, the log amplitude covariance is not directly obtained by cross-correlation of the signal from the detector elements.

For a real detector operating at optical frequencies the detector response is typically proportional to the intensity and it is the covariance of intensity

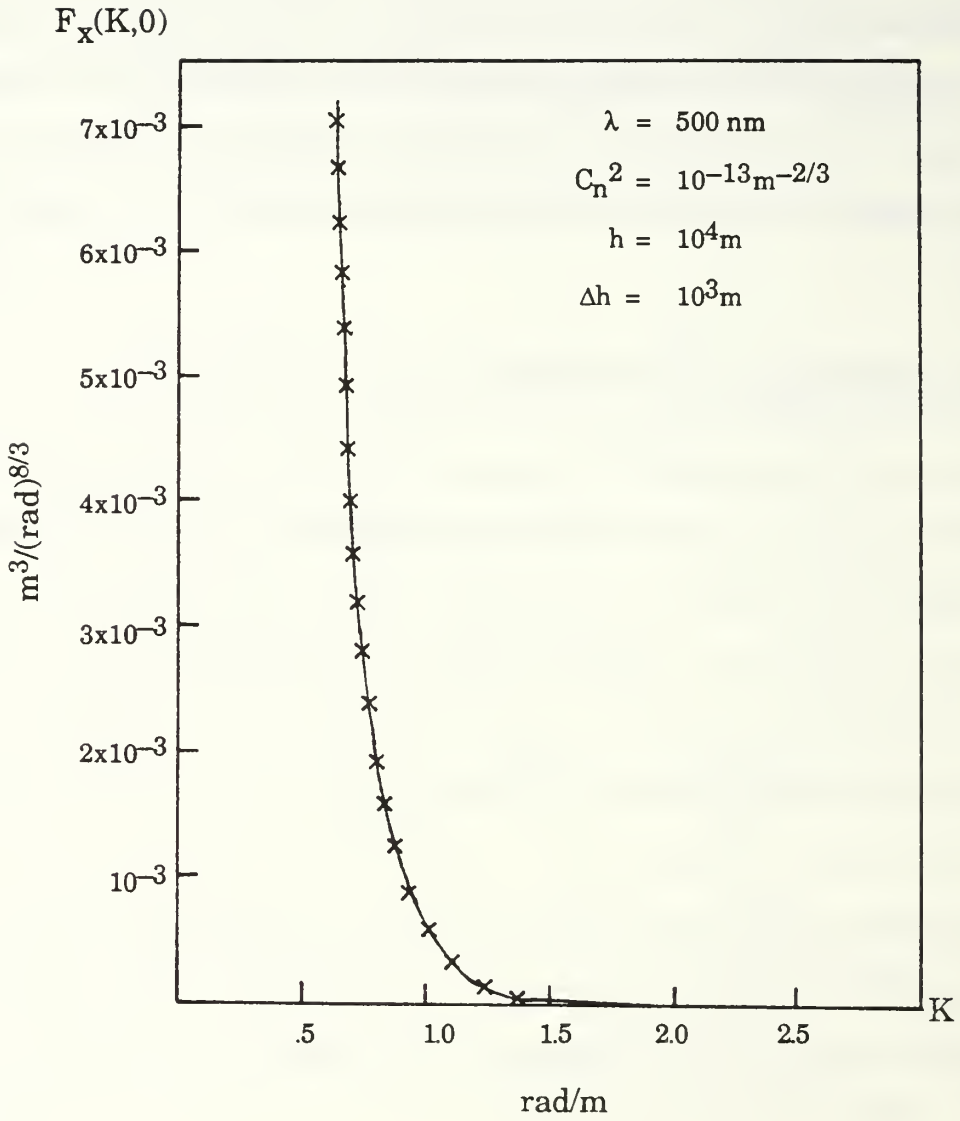

Figure 2. The French Spectrum (x), and the Spectrum of Equation 3.19 (–)

fluctuations that is probed by the detector system. The details of the detection process will be treated in later sections; however, the intensity scintillations in the aperture are independent of the detection process. The spatioangular covariance of intensity fluctuations due to the binary stellar source will now be derived and related to the log amplitude statistics.

1. The Spatial Covariance Functions

For calculational simplicity, consider the wavefronts and two detector elements of Figure 3. The normalized spatial covariance of the intensity is given by:

$$C_I(\rho) = \frac{\left\langle \left[I(\underline{r}_1) - \left\langle I(\underline{r}_1) \right\rangle \right] \left[I(\underline{r}_2) - \left\langle I(\underline{r}_2) \right\rangle \right] \right\rangle}{\left\langle I(\underline{r}_1) \right\rangle \left\langle I(\underline{r}_2) \right\rangle} \tag{3.22}$$

with the angled brackets denoting an ensemble average and $I(\underline{r}_i)$ the instantaneous intensity at $\underline{r}_i$. The sources labeled 1 and 2 are assumed independent; therefore,

$$I(\underline{r}_j) = I_1(\underline{r}_j) + I_2(\underline{r}_j) \tag{3.23}$$

with the subscripts 1 and 2 denoting the sources. Note that conservation of energy requires that the long term average illumination in the exit pupil is uniform. Substituting this expression into equation 3.22 and rearranging terms yields:

$$C_I(\rho) = \left(\left\langle I_1 \right\rangle + \left\langle I_2 \right\rangle \right)^{-2} \left[\left\langle \delta I_1(\underline{r}_1)\, \delta I_1(\underline{r}_2) \right\rangle + \left\langle \delta I_2(\underline{r}_1) \delta I_2(\underline{r}_2) \right\rangle \right.$$
$$\left. + \left\langle \delta I_1(\underline{r}_1)\, \delta I_2(\underline{r}_2) \right\rangle + \left\langle \delta I_1(\underline{r}_2) \delta I_2(\underline{r}_1) \right\rangle \right] \tag{3.24}$$

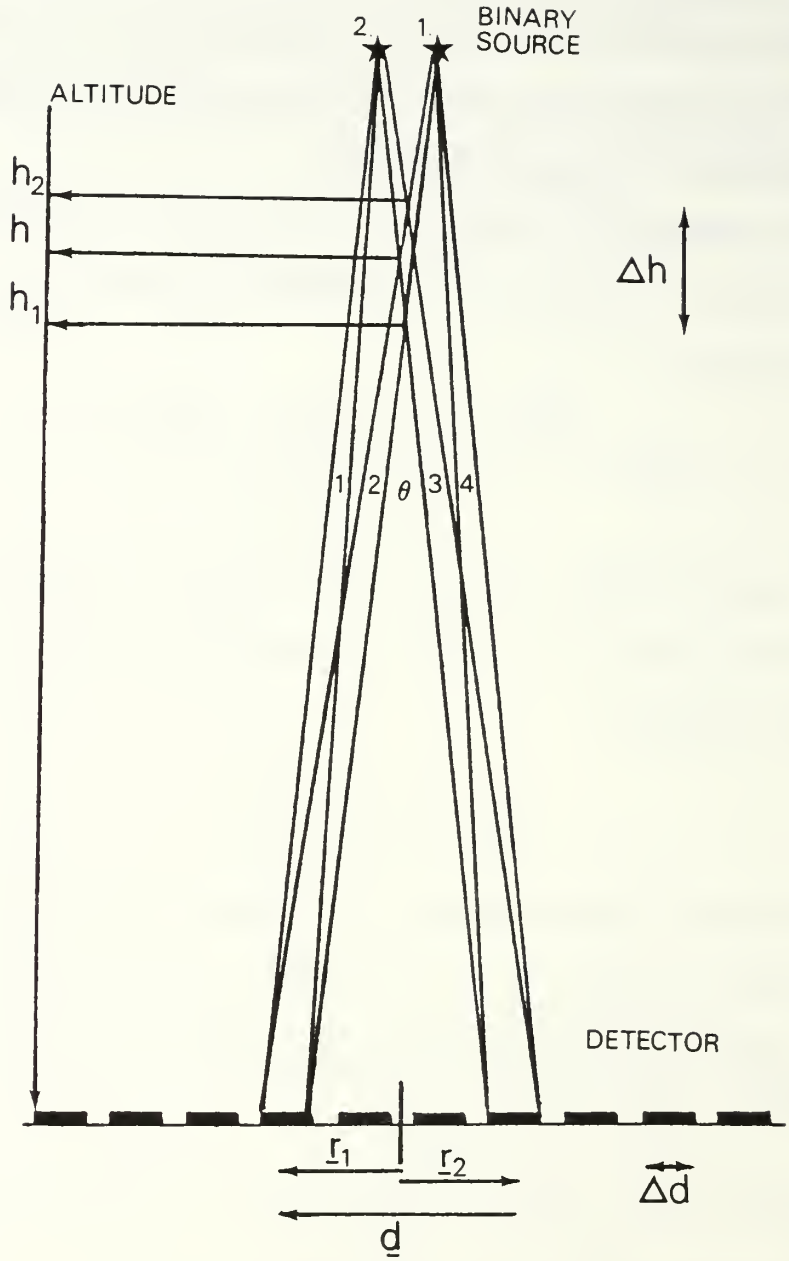

Figure 3. The Wavefronts Intercepted by Detector Elements at r_1, r_2 Due to the Binary Source

with $\delta I = I - \langle I \rangle$. Defining the relative irradiance fluctuations as:

$$l_i(\underline{r}_j) = \frac{\delta I_i(\underline{r}_j)}{\langle I_i(\underline{r}_j) \rangle} \tag{3.25}$$

and substituting into equation 3.24 gives the following expression for the normalized spatial covariance of intensity scintillations:

$$C_I(\rho) = \frac{\langle I_1 \rangle^2}{(\langle I_1 \rangle + \langle I_2 \rangle)^2} \langle l_1(\underline{r}_1)\, l_1(\underline{r}_2) \rangle + \frac{\langle I_2 \rangle^2}{(\langle I_1 \rangle + \langle I_2 \rangle)^2} \langle l_2(\underline{r}_1) l_2(\underline{r}_2) \rangle$$

$$+ \frac{\langle I_1 I_2 \rangle}{(\langle I_1 \rangle + \langle I_2 \rangle)^2} [\langle l_1(\underline{r}_1)\, l_2(\underline{r}_2) \rangle + \langle l_1(\underline{r}_2)\, l_2(\underline{r}_1) \rangle] \tag{3.26}$$

The first two terms of equation 3.26 are the weighted autocovariances of sources 1 and 2 with the weighting functions carrying the brightness or magnitude difference between the two stellar components. Since assuming homogeneity implies that the normalized autocovariances are equal then equation 3.26 is further simplified to:

$$C_I(\rho) = \frac{\langle I_1 \rangle^2 + \langle I_2 \rangle^2}{(\langle I_1 \rangle + \langle I_2 \rangle)^2} \langle l_1(\underline{r}_1)\, l_1(\underline{r}_2) \rangle + \frac{\langle I_1 \rangle \langle I_2 \rangle}{(\langle I_1 \rangle + \langle I_2 \rangle)^2}$$

$$[\langle l_1(\underline{r}_1)\, l_2(\underline{r}_2) \rangle + \langle l_1(\underline{r}_2)\, l_2(\underline{r}_1) \rangle] \tag{3.27}$$

The first term of this equation is the normalized autocovariance of a single source and the second term is the cross covariances of source components 1 and 2.

The intensity covariances in the observation plane are related to the log amplitude covariances by a relation due to Fried [Ref. 23], and since his derivation is clear and readily available it will not be repeated here. In this calculation's notation Fried's result is:

$$C_I(\rho) = \exp[4B_x(\rho)] - 1 \tag{3.28}$$

Since the perturbative solution of the wave equation assumes weak turbulence and this implies that the log amplitude fluctuations are small then equation 3.28 is expanded in a Maclaurin series to first order. The result is:

$$C_I(\rho) \approx 4B_x(\rho) \tag{3.29}$$

Both expressions for the spatial covariance of intensity are graphed in Figure 4 as a function of the log amplitude covariance. The first order approximation is selected for further calculations based on comparison with the experimental curve of Figure 4. As is evident from Figure 4 experimental evidence indicates that the intensity covariance saturates to unity as the intensity of turbulence increases. Therefore, the first order approximation of equation 3.29 is actually a better approximation over the range of validity of the single scattering theory. [Ref. 24]

Using equation 3.29 and examining the terms of equation 3.27 individually then the spatial covariance of intensity scintillations can be cast in a more transparent form in terms of the log amplitude covariance. For the first or autocovariance term of equation 3.27, direct substitution of equation 3.29 yields:

$$\langle l_1(\underline{r}_1)\, l_1(\underline{r}_2)\rangle = 4B_{x_1}(\rho) = 4B_{x_2}(\rho) \tag{3.30}$$

However, the cross covariance terms are not treated as straightforwardly.

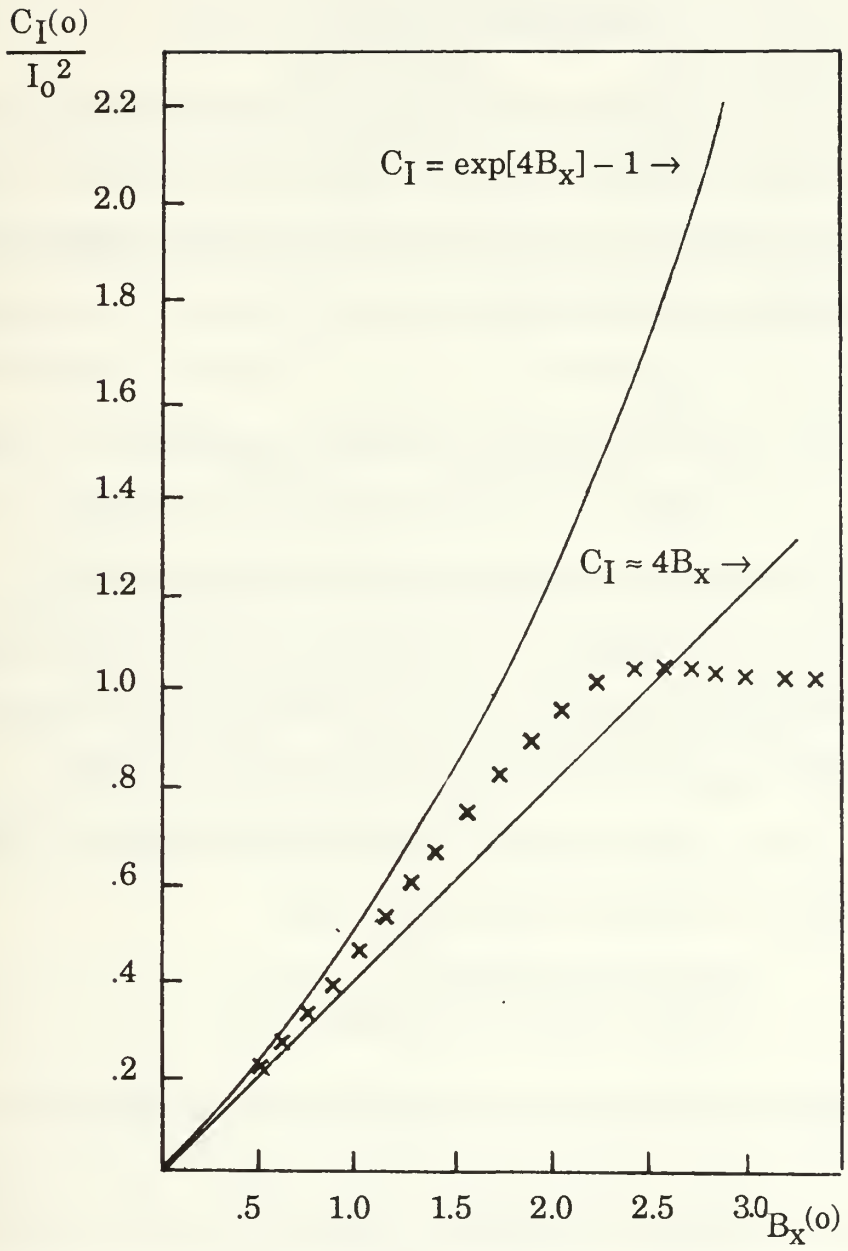

Figure 4. The Normalized Variance of Intensity Scintillations Versus the Log Amplitude Variance for Various Forms for C_I, and Experimental Data Points (x)

The first cross term in equation 3.27 is expressed as a function of the log amplitude using equation 3.29:

$$\langle l_1(\underline{r}_1) l_2(\underline{r}_2) \rangle = 4B_{x_{2,3}}(\rho) \tag{3.31}$$

This term is the cross covariance of the light propagating along the paths labeled by the numbers 2 and 3 in Figure 3. Using equations 2.31 to 2.33 and the assumption of statistical homogeneity then the cross covariance of log amplitude fluctuations is expressed as:

$$B_{x_{2,3}}(\rho) = \int_{-\infty}^{\infty} \exp\left[i\underline{K}\bullet[(\underline{r}_2 - \underline{r}_1) + \rho]\right] F_x(K,0) d^2K \tag{3.32}$$

The assumption of statistical homogeneity in the layer Δh implies that fluctuations in x_1 are mirrored by fluctuations in x_2 at the crossing. Further simplification of equation 3.32 is achieved by using equation 3.1. Substituting this relation between the mean altitude and the detector separation in equation 3.32, this cross term becomes the same function as the autocorrelation but with the origin shifted by θh:

$$B_{x_{2,3}}(\rho) = B_x(\rho - \theta h); \quad \underline{r}_2 - \underline{r}_1 = -\theta h \tag{3.33}$$

An exactly analogous derivation for the second cross term yields:

$$B_{x_{1,4}}(\rho) = B_x(\rho + \theta h); \quad \underline{r}_1 - \underline{r}_2 = \theta h \tag{3.34}$$

That is light propagating along paths 1 and 4 in Figure 3 have a maximum in the spatial covariance for refractive index inhomogeneities with a scale of θh.

Substituting equations 3.33 and 3.34 in equation 3.27 then the spatial covariance of intensity scintillations is expressed as:

$$C_I(\rho) = \frac{\langle I_1\rangle^2 + \langle I_2\rangle^2}{\left[\langle I_1\rangle + \langle I_2\rangle\right]^2} 4B_x(\rho) + \frac{\langle I_1\rangle \langle I_2\rangle}{\left[\langle I_1\rangle + \langle I_2\rangle\right]^2}$$
$$\bullet\ 4\left[B_x(\rho-\theta h) + B_x(\rho+\theta h)\right] \qquad (3.35)$$

with the log amplitude covariance given by the two dimensional Fourier transform of the power spectrum of equation 3.21. Also note that equation 3.35 depends explicitly on θ and the covariance is now called the spatio-angular covariance as a remainder of this dependence.

2. Evaluation of the Spatioangular Covariances

The normalized spatial covariance of equation 3.35 indicates that this intensity expression can be constructed from the log amplitude auto-covariance by appropriate scalings and corresponding shifts of the origin.

Using the Wiener-Khinchin theorem the log amplitude autocovariance in the aperture plane is given by:

$$B_x(\rho) = \int_{-\infty}^{\infty} \exp\left[i\underline{K}\bullet\underline{\rho}\right] F_x(K,0)d^2\underline{K} \qquad (3.36)$$

with the power spectrum given by equation 3.21, and letting the average spectrum condition be understood. Note that $\langle C_n^2(\eta)\rangle$ is now identified as the mean or effective structure parameter in the layer at a mean altitude of h. Equation 3.36 is the two-dimensional Fourier transform of the power spectrum. However, the assumption of isotropy and an assumption of a circular aperture imply that equation 3.36 can be recast as a Hankel transform:

circular aperture imply that equation 3.36 can be recast as a Hankel transform:

$$B_x(\rho) = 2\pi \int_0^\infty F_x(K,0) J_0(K\rho) K dK \tag{3.37}$$

with $J_0(\ )$ the zeroth order Bessel function. Substituting from equation 3.21, the autocovariance becomes:

$$B_x(\rho) = M \int_0^\infty J_0(K\rho)\, K^{-8/3} \sin^2\left(\frac{K^2\eta}{2k}\right) dK \tag{3.38}$$

with $M=4\pi^2(.033)k^2\Delta h\langle C_n^2\rangle$. Note that this integral is valid only for the inertial subrange of spatial scales since the power spectrum is divergent at the origin. Therefore, the limits of integration are changed to $K'=2\pi/L_0$ and $k''=2\pi/l_0$, with l_0 and L_0 the inner and outer scales respectively.

In the limit that ρ goes to zero then equation 3.38 becomes:

$$B_x(o) = M \int_{K'}^{K''} K^{-8/3} \sin^2\left(\frac{K^2 h}{2k}\right) dK \tag{3.39}$$

and this expression is the variance of the log amplitude fluctuations. If $\sqrt{\lambda h}$, with λ the EM wavelength, is much greater than unity then the limits of integration may be extended from zero to infinity with little error [Ref. 18]. Equation 3.39 becomes:

$$B_x(0) = M \int_0^\infty K^{-8/3} \sin^2\left(\frac{K^2 h}{2k}\right) dK \tag{3.40}$$

and this expression has been evaluated by Tatarski in Chapter 8 of Reference 18. In the notation of this calculation the variance of log amplitude fluctuations for the layer at a mean altitude of h is given by:

$$B_x(0) = .564\,\Delta h\, h^{5/6}\, k^{7/6} \langle C_n^2 \rangle \tag{3.41}$$

The integral of equation 3.38 is not analytic and a numerical integration must be carried out to find the spatial covariance. Normalizing equation 3.38 by the variance and carrying out a numerical integration yields the function of Figure 5 with ρ measured in units of $\sqrt{\lambda h}$. [Ref. 19]

The intensity spatial covariance is constructed by appropriate shifting and scaling of the log amplitude covariance as indicated by equation 3.35. Assuming that the components of the binary source are of equal intensity then equation 3.35 becomes:

$$C_I(\rho) = 2B_x(\rho) + \left[B_x(\rho-\theta h) + B_x(\rho+\theta h)\right] \tag{3.42}$$

Normalizing each term of this equation separately:

$$c_I(\rho) = 2b_x(\rho) + b_x(\rho+\theta h) + b_x(\rho-\theta h) \tag{3.43}$$

with $b_x(\rho\pm\theta h)=B_x(\rho\pm\theta h)/B_x(0)$. A graph of this function for h of ten kilometers is constructed in Figure 6 with ρ,h scaled by $\sqrt{\lambda h}$.

For experimental implementation the needed covariance functions could be computed beforehand and stored for later use. Another alternative would be to find a suitable Chebyshev polynomial expansion of the integral of equation 3.38. However, the effects of nonideal optics must be considered and this implies a numerical calculation of the log amplitude autocovariance.

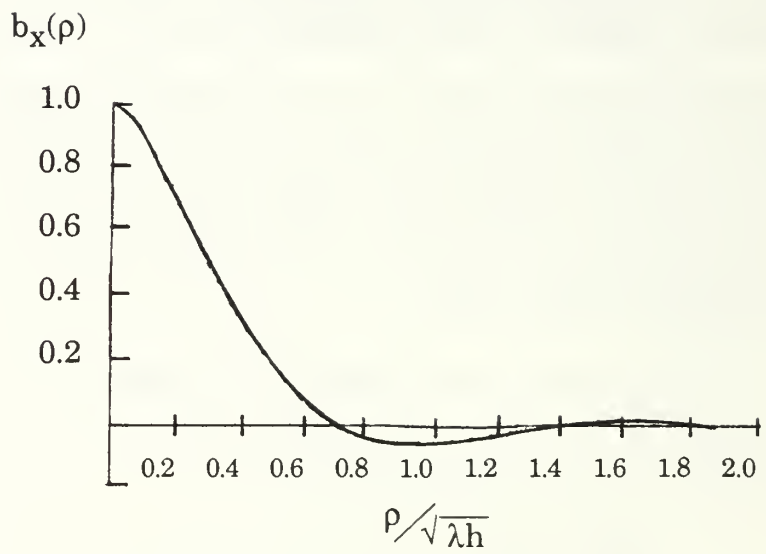

Figure 5. The Normalized Log Amplitude Spatial Covariance of Fluctuations [Ref. 19]

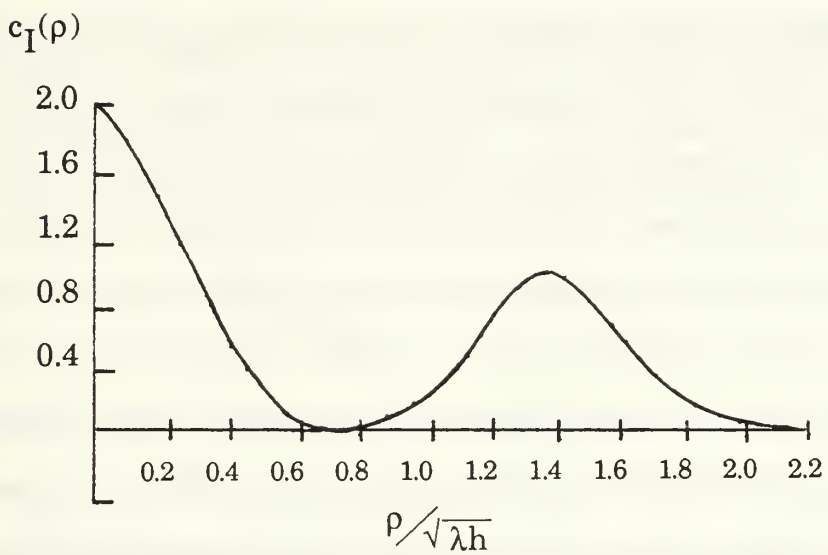

Figure 6. The Normalized Spatial Covariance of Intensity Scintillations

3. Nonideal Optical Corrections to the Autocovariance

The actual detector system is coupled to an optical system with the real detector array in the exit pupil. Taking the linear systems viewpoint of the optical system then it is viewed as a linear transformation of the optical input at the aperture. The individual spatial frequencies in the aperture are transformed to the exit pupil via the optical transfer function (OTF). The OTF of the optical system is defined as the ratio of the output spatial power spectrum to the input spectrum, and it is a spatial frequency dependent complex quantity with the modulus defining the modulation transfer function (MTF) and phase, the phase transfer function (PTF). The optical system is assumed on axis and since phase shifts in centered optical systems occur off axis then the MTF is the quantity of interest. The MTF describes the filtering of spatial frequencies by the optical system. For the detector array in the exit pupil a spatially modulated input will result in a spatially modulated output that is suitably scaled; however, if the MTF falls to zero (optical system cutoff) rapidly or is a rapidly varying function of spatial frequency then the output spatial spectrum is found from

$$F_x(K,0) \Big|_{output} = MTF(K)\, F_x(K,0) \Big|_{input} \tag{3.44}$$

by the definition of the OTF. The spatial autocovariance then becomes the Hankel transform of equation 3.44 as indicated in the previous section.

The power spectrum of log amplitude fluctuations in the aperture is illustrated in Figure 2 and it is noted that this spectrum falls rapidly to zero as a function of spatial frequency. Therefore, the assumption of unity MTF is quite good for reasonable aperture sizes (greater than approximately 20 cm). The MTF will be assumed constant for the balance of this

calculation; however, experimental implementation of this scheme should include a measurement of the MTF of the optical system.

With the assumption of constant MTF over the inertial subrange, the scaling between the aperture and exit pupil is derived from geometrical considerations. As is apparent from Figure 7 the average intensity in the exit pupil is increased by the factor:

$$T_r D_A^2 \Big/ D_E^2 \tag{3.45}$$

with D_A the aperture diameter, D_E the diameter of the exit pupil and T_r the overall transmittance of the optical system. For the linear detector array illustrated, the scaled array in the aperture is characterized by:

$$A_A = A_E \, D_A^2 \Big/ D_E^2 \quad ; \quad \rho_A = \rho_E \, D_A \Big/ D_E \tag{3.46}$$

with A the detector element area, ρ a linear displacement along the array and the subscripts A and E referring to the aperture and exit pupil respectively. For the remainder of this calculation the optical system coupled to the detector is assumed to have unity transmittance and constant MTF over the inertial subrange. Under these assumptions the covariances of the previous section are assumed valid.

Given the assumption of an ideal optical system the interaction of the electromagnetic field with the detector elements must now be considered. The next section discusses the photon counting statistics of the binary source profiling method.

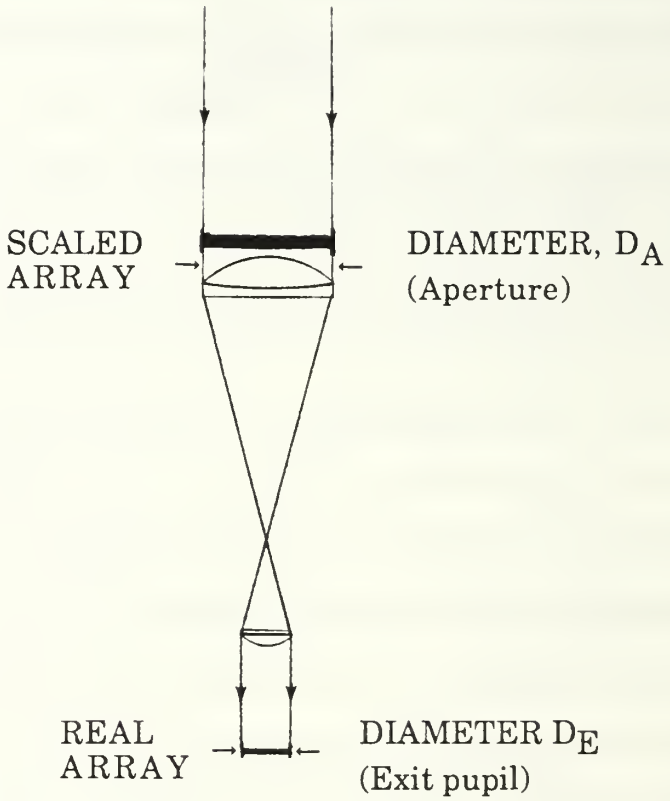

Figure 7. An idealized Optical System Illustrating the Scaling Between Aperture and Exit Pupil Plane

IV. PHOTOELECTRON COUNTING STATISTICS

The intensity scintillations are detected by a linear array of photosensitive or photoemissive detectors, and the discrete nature of this detection process must be considered. The incident electromagnetic flux causes the photosensitive surface of a detector element to eject a photoelectron and these electrons are then collected and analyzed as the detector element signal. Following Saleh [Ref. 25], this derivation treats the electromagnetic field classically as a stochastic quantity; and, the photoelectron production process is treated semiclassically. This approach does not invoke the photon concept and has the advantage of not demanding the full quantum electrodynamic treatment of the electromagnetic field. The semiclassical approach is compatible with the full quantum analysis of the photoemission process provided certain mildly restrictive assumptions hold true. [Ref. 25]

To proceed with this analysis a certain amount of statistical background is required. The definitions and relations used in this calculation are summarized in the next section and the notation used is that of Reference 25.

A. STATISTICAL BACKGROUND

For an experiment that counts photoelectrons the observed data is the number of counts $(n_1,n_2,...n_m)$ in the intervals (t_J,t_J+T) with J equal to (1,2,...m). Since the photoemission process is assumed probabilistic, the number of counts in disjoint time intervals are assumed independent. Therefore, a rate density $\beta(t)$ is defined:

$$\beta(t) = \lim_{\Delta t \to 0} \frac{\langle N_t(t + \Delta t) - N_t(t) \rangle}{\Delta t} \tag{4.1}$$

with $N_T(t)$ the number of events in the interval T. This function is also known as the arrival rate of a Poisson process [Ref. 26].

Given an assumption of independence in disjoint intervals then the process described is called a Poisson point process (P.PP) with rate density $\beta(t)$. The number of points (counts) in a single interval (t,t+T) has a Poisson density:

$$P(n) = \frac{W^n}{n!} \exp(-W) \tag{4.2}$$

with W, the integrated rate of events defined by the relation:

$$W = \int_{t_o}^{t_o+T} \beta(t)\, dt \tag{4.3}$$

And, the time T is the counting time. If β is a constant then the P.PP is called homogeneous and equation 4.2 becomes:

$$P(n) = \frac{(\beta T)^n}{n!} \exp(-\beta T) \tag{4.4}$$

The integer random variable n is also described statistically by the moment generating function (mgf). The ordinary moment generating function is defined by:

$$Q_n(s) = \langle \exp(-ns) \rangle = \sum_{n=o}^{\infty} \exp(-ns)\, P(n) \tag{4.5}$$

with P(n) given by equation 4.2. Carrying out the indicated summation using equation 4.2 gives the following expression for the mgf:

$$Q_n(s) = \exp\left[W(\exp(-s) - 1)\right] \tag{4.6}$$

The usefulness of the mgf is apparent when the term exp(-ns) is expanded in a Maclaurin series. The mth term of the expansion evaluated at s = 0 is the mth ordinary moment of n. Using equation 4.2 and the mgf the relations between the moments of W and n are easily derived. Several of these are listed here for future reference:

- ordinary moments

$$\begin{aligned} &\langle n\rangle = W && \text{a)} \\ &\langle n^2\rangle = W^2+W && \text{b)} \\ &\langle n_1 n_2\rangle = W_1 W_2 && \text{c)} \end{aligned} \tag{4.7}$$

- central moments

$$\begin{aligned} &\langle \delta n\rangle = \langle (n-\langle n\rangle)\rangle = 0 && \text{a)} \\ &\langle (\delta n)^2\rangle = W && \text{b)} \\ &\langle \delta n_1 \delta n_2\rangle = 0 && \text{c)} \end{aligned} \tag{4.8}$$

The statistics of a non-homogeneous P.PP are completely determined by the rate density $\beta(t)$. However, if $\beta(t)$ is itself a stochastic function then the statistics of the point process depend on the statistics of β. If $\beta(t)$ is a stationary stochastic function then the point process described by it is called a doubly stochastic Poisson point process (DSP.PP). The moments and moment generating functions of the DSP.PP are found by averaging the corresponding moments and mgf's of the P.PP over the different realizations of $\beta(t)$ or the integrated rate W. Thus, the moments of the DSP.PP are obtained by averaging equation 4.7 over W. They are listed here:

- ordinary moments of DSP.PP

$$\begin{aligned} &\langle n\rangle = \langle W\rangle && \text{a)} \\ &\langle n^2\rangle = \langle W^2\rangle+\langle W\rangle && \text{b)} \end{aligned} \tag{4.9}$$

and, conversely:

$$\langle W \rangle = \langle n \rangle \qquad \text{a)}$$
$$\langle W^2 \rangle = \langle n^2 \rangle - \langle n \rangle \qquad \text{b)} \tag{4.10}$$

Also:

$$\langle n_1 n_2 \rangle = \langle W_1 W_2 \rangle \tag{4.11}$$

- variance of DSP.PP

$$\langle (\delta n)^2 \rangle = \langle (\delta W)^2 \rangle + \langle W \rangle \tag{4.12}$$

These relations and the results of section III are used to derive the photoelectron counting statistics for the binary source method.

B. THE RATE OF PHOTOEMISSIONS

A full quantum analysis of the photoemission process reveals the following facts [Ref. 25]:

1. The probability of transition from a bound to an unbound state for an electron in a photosensitive surface during a time Δt is proportional to Δt and the instantaneous intensity.

2. If the intensity is a stochastic function of time then the photoemission process is a DSP.PP.

These conditions hold quite generally if the following two auxiliary conditions hold:

1. The time Δt, though much greater than the period of oscillation of the EM wave, is much shorter than other characteristic time scales of the experiment.

2. The bandwidth of unbound (free) electron states is much greater than the EM bandwidth.

Under these conditions then the rate density of photoelectric emissions can be expressed as:

$$\beta(t,\underline{r}) = \iint_{\nu,A_D} d\nu\, d^2\underline{r}\, \alpha(\nu)\, I(\underline{r},t,\nu) \tag{4.13}$$

with ν the EM frequency, A_D the detector element area and $\alpha(\nu)$ the quantum efficiency at frequency ν.

This expression for the rate density is simplified by making the quasimonochromatic approximation. The quasimonochromatic approximation assumes that the center EM frequency is much greater than the EM bandwidth. For optical frequencies this condition is easily satisfied by using an appropriate set of colored filters. However, the same thing is accomplished by a narrowband detector response. If a more accurate assessment of the frequency dependence is required the stellar spectrum is modeled by a Planck blackbody spectrum and the explicit frequency dependence of the quantum efficiency is used to evaluate the frequency integral of equation 4.13. However, since an analytic form for the quantum efficiency is not readily available this calculation proceeds by invoking the quasimonochromatic approximation and approximating the frequency integral as follows:

$$\beta(\underline{r},t) = \Delta\nu\, \alpha(\nu_o) \int_{A_D} d^2\underline{r}\, I(\underline{r},t,\nu_o) \tag{4.14}$$

with ν_o the center frequency.

The spatial integral can similarly be approximated by assuming that the area over which the spatial fluctuations are correlated is much larger than the detector element area. The rate density then becomes:

$$\beta(\underline{r}_i,t) = \Delta\nu\, \alpha(\nu_o)\, A_D\, I(\underline{r}_i,t,\nu_o) \tag{4.15}$$

with r_i the geometric center of the detector element.

The rate of photoemissions is given by equation 4.3:

$$W(\underline{r}_i,t) = \int_t^{t+T} \beta(t,\underline{r}_i)dt = \gamma \int_t^{t+T} I(r_i,t)\, dt \tag{4.16}$$

with γ equal to $\Delta\nu\alpha(\nu_0)A_D$ and letting the frequency dependence be understood. But, as noted in section III, the intensity is the sum of two independent sources:

$$I(\underline{r}_i,t) = I_1(\underline{r}_i,t) + I_2(\underline{r}_i,t) \tag{4.17}$$

Following Fried [Ref. 23], the intensity is expressed as a function of the log amplitude as:

$$I_j(\underline{r}_i,t) = I_j^o(t)\, \exp\left(2x_j(\underline{r}_i,t)\right) \tag{4.18}$$

with $I_i^o(t)$ the source intensity; and, the exponential term is the atmospheric modulation. Again, the source term is assumed spatially, though not temporally, coherent over the detector element area. Under these assumptions the rate is:

$$W(\underline{r}_i,t) = \gamma \int_t^{t+T} \left[I_1^o(t)\, \exp\left(2x_1(r_i,t)\right) + I_2^o(t)\exp\left(2x_2(r_i,t)\right)\right]dt \tag{4.19}$$

The stellar sources are assumed thermal and as is well known thermal sources have a coherence time that is the inverse of the optical bandwidth. However, the correlation time associated with the atmospheric modulation is on the order of one millisecond. This is consistent with the assumption of frozen turbulence for times less than or equal to one millisecond [Ref. 20]. For any reasonable optical bandwidth the source coherence time is safely assumed to be many orders of magnitude less than the correlation time of

the atmospheric modulation. Selecting an integration time that is much less than the atmospheric correlation time and much greater than the source coherence time the rate becomes:

$$W(\underline{r}_i,t_j) = W_1^0(t_j)\exp\left(2x_1(r_i,t_j)\right) + W_2^0(t_j)\exp\left(2x_2(r_i,t_j)\right) \qquad (4.20)$$

with $t_j = t+T/2$. Note that the atmospheric modulation is considered frozen over the integration time.

Equation 4.20 is used to form the second order moments of the rate and these moments are related to the second order moments of the photoelectron counts.

C. COVARIANCE OF PHOTOELECTRON COUNTS

Forming the normalized spatial covariance of the integrated rate yields:

$$\frac{\langle \delta W(r_1,t_i)\,\delta W(r_2,t_i)\rangle}{\langle W(r_1,t_i)\rangle\langle W(r_2,t_i)\rangle} = \frac{\langle W(r_1,t_i)\,W(r_2,t_i)\rangle}{\langle W(r_1,t_i)\rangle\langle W(r_2,t_i)\rangle} - 1 \qquad (4.21)$$

with the angled brackets denoting an ensemble average. Examining the correlation term of equation 4.21 and noting that the atmospheric and source modulation are independent then this term becomes:

$$\begin{aligned}\langle W(r_1,t_i)\,W(r_2,t_i)\rangle &= \langle W_1^0(t_i)\rangle\langle\exp[2x_1(r_1,t_i) + 2x_1(r_2,t_i)]\rangle \\ &+ \langle W_2^0(t_i)\rangle\langle\exp[2x_2(r_1,t_i) + 2x_2(r_2,t_i)]\rangle + \langle W_1^0(t_i)\,W_2^0(t_i)\rangle \\ &\cdot \{\langle\exp[2x_1(r_1,t_i) + 2x_2(r_2,t_i)]\rangle + \langle\exp[2x_1(r_2,t_i) + 2x_2(r_1,t_i)]\rangle\} \qquad (4.22)\end{aligned}$$

by using equation 4.20. This relation is further simplified by using the relation between the intensity and the log amplitude. Following Fried

[Ref. 23], the exponential terms of equation 4.22 are related to the log amplitude covariance by:

$$\left\langle \exp\left[2x_i(r_e,t_k) + 2x_j(r_m,t_k)\right]\right\rangle = \exp\left[4B_{x_{i,j}}(\rho)\right] \tag{4.23}$$

Since the log amplitude fluctuations are assumed small then this expression is expanded in a Maclaurin series to yield:

$$\exp\left[4B_{x_{i,j}}(\rho)\right] \approx 4B_{x_{i,j}}(\rho) + 1 \tag{4.24}$$

The various log amplitude covariances implied by equation 4.24 are again simplified by appealing to the symmetry of Figure 3 and equations 3.31 to 3.34. The result is:

$$\begin{aligned}\left\langle W(r_1,t_i)\, W(r_2,t_i)\right\rangle &= \left[\left\langle W_1^o(t_i)^2\right\rangle + \left\langle W_2^o(t_i)^2\right\rangle\right]\left(4B_x(\rho)+1\right) \\ &+ 4\left\langle W_1^o(t_i)\, W_2^o(t_i)\right\rangle\left[B_x(\rho-\theta h) + B_x(\rho+\theta h)\right]\end{aligned} \tag{4.25}$$

or, rearranging terms:

$$\begin{aligned}\left\langle W(r_1,t_i)W(r_2,t_i)\right\rangle &= \left\langle\left[W_1^o(t_1)+W_2^o(t_i)\right]^2\right\rangle + \left[\left\langle W_1^o(t_i)^2\right\rangle+\left\langle W_2^o(t_i)^2\right\rangle\right]4B_x(\rho) \\ &+ 4\left\langle W_1^o(t_i)W_2^o(t_i)\right\rangle\left[4B_x(\rho-\theta h) + 4B_x(\rho+\theta h)\right]\end{aligned} \tag{4.26}$$

Noting that $\langle\exp[2x(\underline{r},t)]\rangle$ equals unity by conservation of energy then the normalizing term of equation 4.21 is expressed as:

$$\left\langle W(r_1,t_i)\right\rangle\left\langle W(r_2,t_i)\right\rangle = \left[\left\langle W_1^o(t_i)\right\rangle + \left\langle W_2^o(t_i)\right\rangle\right]^2 \tag{4.27}$$

by using equation 4.20. Therefore, substituting from equations 4.26 and 4.27 in equation 4.21 yields the following expression for the spatial covariance of the rate:

$$\frac{\langle \delta W(r_1,t_i)\, \delta W(r_2,t_i)\rangle}{\langle W(r_1,t_i)\rangle\langle W(r_2,t_i)\rangle} = \frac{\langle [W_1^o(t_i) + W_2^o(t_i)]^2\rangle}{[\langle W_1^o(t_i)\rangle + \langle W_2^o(t_i)\rangle]^2}$$

$$\frac{[\langle W_1^o(t_i)^2\rangle + \langle W_2^o(t_i)^2\rangle]}{[\langle W_1^o(t_i)\rangle + \langle W_2^o(t_i)\rangle]^2} 4B_x(\rho) + \frac{4\langle W_1^o(t_i)\, W_2^o(t_i)\rangle}{[\langle W_1^o(t_i)\rangle + \langle W_2^o(t_i)\rangle]^2}$$

$$\bullet\, [B_x(\rho+\theta h) + B_x(\rho-\theta h)] - 1 \qquad (4.28)$$

As stated previously the photoelectron emission process is a DSP.PP for a stochastic intensity. The relations between the second order moments of W, the integrated rate and n, the number of counts, are given by equations 4.9 to 4.12. Substituting from these relations in the rate spatial covariance of equation 4.28 yields:

$$\frac{\langle \delta n(r_1,t_i)\, \delta n(r_2,t_i)\rangle}{\langle n(r_1,t_i)\rangle\langle n(r_2,t_i)\rangle} = \frac{\langle [n_1(t_i) + n_2(t_i)]^2\rangle}{[\langle n_1(t_i)\rangle + \langle n_2(t_i)\rangle]^2} - \frac{[\langle n_1(t_i)\rangle + \langle n_2(t_i)\rangle]}{[\langle n_1(t_i)\rangle + \langle n_2(t_i)\rangle]^2} - 1$$

$$+ \frac{[\langle n_1(t_i)^2\rangle + \langle n_2(t_i)^2\rangle - \langle n_1(t_i)\rangle - \langle n_2(t_i)\rangle]}{[\langle n_1(t_i)^2\rangle + \langle n_2(t_i)\rangle]^2} 4B_x(\rho)$$

$$+ \frac{4\langle n_1(t_i)\rangle\, \langle n_2(t_i)\rangle}{[\langle n_1(t_i)\rangle + \langle n_2(t_i)\rangle]^2} [B_x(\rho-\theta h) + B_x(\rho+\theta h)] \qquad (4.29)$$

This is the normalized spatial covariance of photoelectron counts for a binary stellar source.

To proceed further note that a single measurement or counting interval T of approximately one millisecond probes a single configuration of the atmospheric modulation. This single measurement is clearly insufficient to determine the modulation statistics, and since there is only one

atmosphere to sample then the ensemble averages of equation 4.29 must be replaced with a time average. Assuming ergodicity holds, Saleh [Ref. 28] points out that long time averages wash out the stochastic nature of the intensity fluctuations. To demonstrate this assume that the unmodulated source intensity is characteristic of linearly polarized thermal light. Saleh derives the probability density of photoelectron counts in terms of the parameter N:

$$P(n) = \binom{n+N-1}{n} \left(1 + \frac{\langle n \rangle}{N}\right)^{-N} \left(1 + \frac{N}{\langle n \rangle}\right)^{-n} \tag{4.30}$$

with N the number of coherence times of the source intensity. Apparently, a good determination of the atmospheric modulation is made only after many coherence times of the source intensity have elapsed. In the limit that N goes to infinity equation 4.30 becomes the Poisson distribution:

$$P(n) = \frac{\langle n \rangle^h}{n!} \exp\left(-\langle n \rangle\right) \tag{4.31}$$

And as is well known [Ref. 26], the following relations hold for the Poisson distribution:

$$\left\langle (\delta n)^2 \right\rangle = \left\langle n \right\rangle \tag{4.32}$$

$$\left\langle n^2 \right\rangle = \left\langle n \right\rangle^2 + \left\langle n \right\rangle \tag{4.33}$$

Therefore in the limit of long (compared with one millisecond) time averages the normalized spatial covariance of counts is:

$$\frac{\langle \delta n(r_1,t_i)\delta n(r_2,t_i)\rangle}{\langle n(r_1,t_i)\rangle\langle n(r_2,t_i)\rangle} = \frac{\langle n_1\rangle^2 + \langle n_2\rangle^2}{[\langle n_1\rangle + \langle n_2\rangle]^2} 4B_x(\rho) + \frac{4\langle n_1\rangle\langle n_2\rangle}{[\langle n_1\rangle + \langle n_2\rangle]^2}$$

$$\bullet \left[B_x(\rho-\theta h) + B_x(\rho+\theta h)\right] \qquad (4.34)$$

This expression indicates that the spatial covariance of counts is directly dependent on the second order statistics of the atmospheric modulation. The source modulation is averaged away due to the extremely short ($\Delta\nu \geq 10^8$Hz) coherence time of the source radiation.

Since the actual experiment depends on replacing ensemble averages with time averages the statistics of the experimentally estimated spatial covariance must be explored. The next section examines the counting experiment for a single layer Δh.

D. STATISTICAL ACCURACY

The spatial covariance of counts:

$$\frac{\langle \delta n(r_1,t_i)\, \delta n(r_2,t_i)\rangle}{\langle n(r_1,t_i)\rangle\, \langle n(r_2,t_i)\rangle} = \frac{\langle n(r_2,t_i)\, n(r_1,t_i)\rangle}{\langle n(r_1,t_i)\rangle\, \langle n(r_2,t_i)\rangle} - 1 \qquad (4.35)$$

can be estimated by the expression:

$$\hat{g} = \frac{\hat{G}}{\hat{n}(r_1)\,\hat{n}(r_2)} - 1 \qquad (4.36)$$

with;

$$\hat{G} = \frac{1}{N}\sum_{m=1}^{N} n(r_1,t_m)\, n(r_2,t_m) \;;\; \hat{n}(r_j) = \frac{1}{N}\sum_{m-1}^{N} n(r_j,t_m) \qquad (4.37)$$

N is the number of counting intervals of length T, and T is expected to be much longer than the source coherence time and less than the atmospheric modulation correlation time. The estimator $\hat{g}$ is characterized by its mean and variance. The mean or expected value of g is apparently given by equation 4.34.

$$\langle \hat{g} \rangle = \frac{\langle n_1 \rangle^2 + \langle n_2 \rangle^2}{[\langle n_1 \rangle + \langle n_2 \rangle]^2} 4B_x(\rho) + \frac{4\langle n_1 \rangle \langle n_2 \rangle}{[\langle n_1 \rangle + \langle n_2 \rangle]^2} \cdot [B_x(\rho - \theta h) + B_x(\rho + \theta h)] \tag{4.38}$$

However, the variance of g is a difficult quantity to derive. The variance of g is defined by the relation:

$$\text{var}(\hat{g}) = \langle (\hat{g} - \hat{g})^2 \rangle \tag{4.39}$$

which simplifies to:

$$\text{var}(\hat{g}) = \left\langle \left[\frac{\hat{G}}{\hat{n}(r_1)\hat{n}(r_2)} - \left\langle \frac{\hat{G}}{\hat{n}(r_1)\hat{n}(r_2)} \right\rangle \right]^2 \right\rangle \tag{4.40}$$

This quantity is the same as the variance of the estimated spatial correlation of counts. Saleh evaluates this variance by expanding $\hat{G}$ and $\hat{n}_j$ about their means and retaining only the deviations from these means. With the additional assumption that N is very large the variance of $\hat{g}$ is given by equation 7.181 of Reference 25. In the notation of this calculation, the variance of g is:

$$\mathrm{var}(\hat{g}) = \mathrm{var}(\hat{G})/\left(\langle n(r_1)\rangle\langle n(r_2)\rangle\right) + \Delta$$

$$\Delta = 4\langle\hat{g}\rangle + \sum_{j=1,2}\left[\frac{-2\langle\hat{g}\rangle\langle\hat{G}\hat{n}(r_j)\rangle}{\langle n(r_1)\rangle\langle n(r_2)\rangle\langle n(r_j)\rangle} + \frac{\langle\hat{g}\rangle^2}{\langle n(r_j)\rangle^2}\,\mathrm{var}(\hat{n}(r_j))\right]$$

$$+ \frac{2\,\mathrm{cov}\left(\langle n(r_1)\rangle, \langle n(r_2)\rangle\right)}{\langle n(r_1)\rangle\,\langle n(r_2)\rangle} \qquad (4.41)$$

with the indicated variances the full spatiotemporal variances of the indicated quantities. Unfortunately, a complete evaluation of this expression requires the time statistics of the atmospheric modulation. The turbulence in the atmosphere is typically intermittent in intensity and the statistics of intermittency are inaccessible with current theoretical models. However, the single scattering assumption allows a lower bound to be placed on the variance of $\hat{g}$.

The time statistics of the evolving refractive index inhomogeneities will depend on moments of the velocity field of higher order than is represented by the structure function (see section II). This implies that the temporal variance of the spatioangular correlation of log amplitude fluctuations will be a quantity that is fourth order in the log amplitude. By the single scattering approximation these moments are approximately zero. Therefore neglecting the terms in the variance of $\hat{g}$ that are of order $\hat{g}^2$ and higher, then equation 4.41 becomes:

$$\mathrm{var}(\hat{g}) \geq 4\langle\hat{g}\rangle + \frac{2\langle\hat{g}\rangle}{\langle n(r_1)\rangle\langle n(r_2)\rangle} = 4\langle\hat{g}\rangle\left[1 + \frac{.5}{\left[\langle n_1\rangle + \langle n_2\rangle\right]^2}\right] \qquad (4.42)$$

with n_1, n_2 the counts due to source 1 and 2 respectively. The relative error is defined as:

$$e = 100 \left[\text{var}\,(\hat{g})\right]^{1/2} / \langle \hat{g} \rangle \tag{4.43}$$

or,

$$e = \frac{200}{\left(\langle \hat{g} \rangle\right)^{1/2}} \left[1 + .5/\left[\langle n_1 \rangle + \langle n_2 \rangle\right]^2\right]^{1/2} \tag{4.44}$$

A graph of the relative error for $\langle n_1 \rangle = \langle n_2 \rangle = n$ is given in Figure 8 as a function of the spatioangular covariance of counts $\langle \hat{g} \rangle$.

From Figure 8, the relative error diverges rapidly as $\langle \hat{g} \rangle$ goes to zero. Since observed values of C_n^2 are very small (10^{-12} to $10^{-14} cm^{1/3}$) [Ref. 12] then the relative error induced due to the detection process will dominate the counting statistics. Clearly some error reduction scheme is required to extract the spatial covariance of counts.

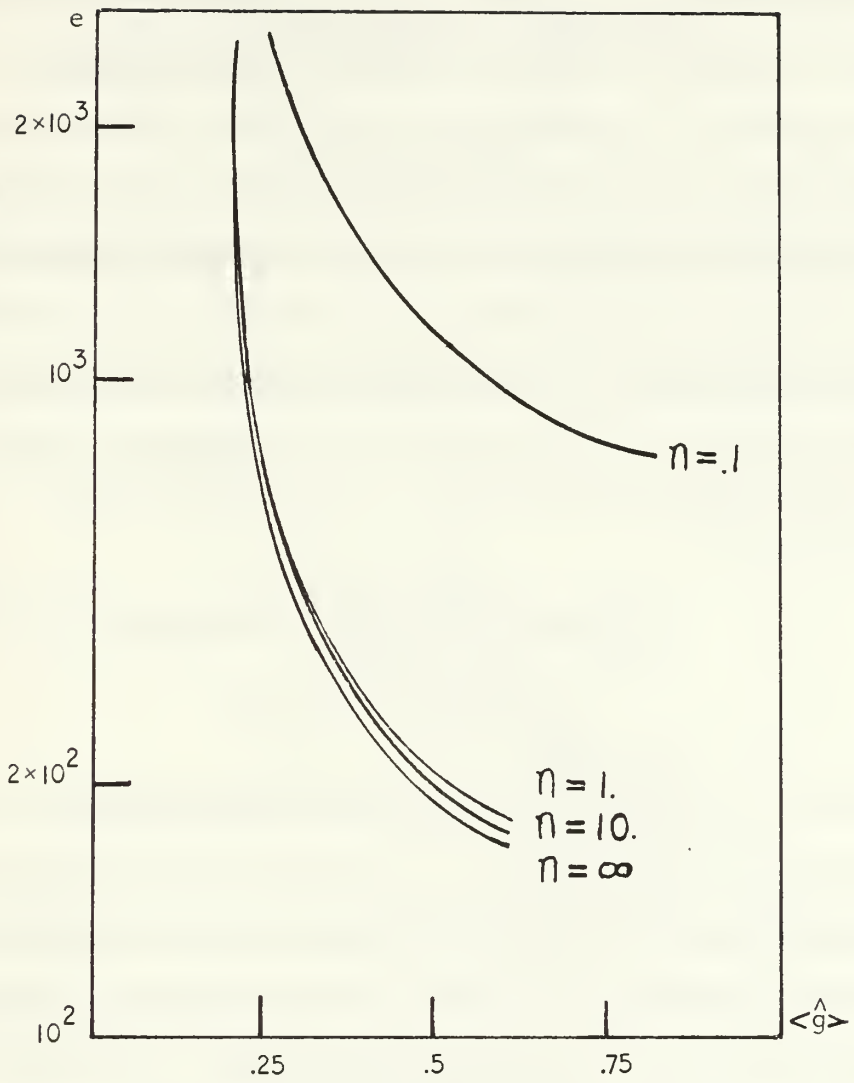

Figure 8. Relative Error Versus Spatioangular Covariance of Counts for Various Values of Incident Intensity

V. LEAST SQUARES ANALYSIS

The analysis of the preceding section indicated the dominance of the detection uncertainty in the determination of the spatioangular covariance. This large error is ameliorated by using the redundant information provided by the multiple detector elements of the array (Figure 3). Least squares analysis is employed to use this redundant information to reduce noise.

Most of the analysis to this point has applied to a single layer at a mean altitude h. However, equation 4.38 is easily generalized to any layer with a mean altitude of h_i:

$$C_n(\rho_j,h_i) = \frac{\langle n_1\rangle^2 + \langle n_2\rangle^2}{[\langle n_1\rangle+\langle n_2\rangle]^2}\ 4\, B_x(\rho_j,h_i) + \frac{4\langle n_1\rangle\langle n_2\rangle}{[\langle n_1\rangle+\langle n_2\rangle]^2}\ [B_x(\rho_j-\theta h_i) + B_x(\rho_j+\theta h_i)] \tag{5.1}$$

Note that the log amplitude covariances are now calculated at the centers of the detector elements ρ_j. With the previous assumption of a small detector element size this is a reasonable approximation. Rewriting the spatioangular weighting functions to reflect the explicit dependence on the refractive index structure parameter yields:

$$B_x(\rho_j,h_i) = \langle C_n^2(h_i)\rangle\, B_x^1(\rho_j,h_i) \tag{5.2}$$

and equation 4.38 is generalized to:

$$C_n(\rho_j,h_i) = \langle C_n^2(h_i)\rangle \left\{ \frac{\langle n_1\rangle^2 + \langle n_2\rangle^2}{[\langle n_1\rangle+\langle n_2\rangle]^2}\, 4B_x^1(\rho_j,h_i) + \right.$$

$$\left. \frac{4\langle n_1\rangle\langle n_2\rangle}{[\langle n_1\rangle+\langle n_2\rangle]^2} [B_x(\rho_j-\theta h_i) + B_x(\rho_j+\theta h_i)] \right\}$$

$$= \langle C_n^2(h_i)\rangle\, R(\rho_j,h_i) \tag{5.3}$$

Using this equation, and assuming the fluctuations induced by non-overlapping layers are uncorrelated, then spatioangular covariance of counts observed in the aperture due to multiple layers is given by the summation:

$$CR(\rho_j) = \sum_{h_i} C_n(\rho_j,h_i) = \sum_{h_i} \langle C_n^2(h_i)\rangle\, R(\rho_j,h_i) \tag{5.4}$$

This summation is equivalent to the matrix equation:

$$[CR_k] = [R_{kj}]\,[(C_n^2)_j] \tag{5.5}$$

with CR_k the experimentally measured spatial covariance of counts, ${C_n}^2{}_j$ the undetermined refractive index structure parameter profile and R_{jk} the weighting functions described above. The undetermined ${C_n}^2$ are found by minimizing the quantity:

$$\left| [CR_k] - [R_{kj}]\,[(C_n^2)_j] \right| = \text{minimum} \tag{5.6}$$

as a function of ${C_n}^2$. The solution to this is well known and is given by:

$$[C_{nj}^2] = ([R_{kj}]^*[R_{kj}])^{-1}[R_{kj}]^*[CR_k] \tag{5.7}$$

with the superscript * denoting the Hermitian conjugate. This process is formally known as least squares analysis and the ${C_n}^2$ vector obtained is the

least squares approximation of the structure parameter profile. A more explicit expression for the profile is obtained by considering the experimentally derived spatioangular covariance.

The experimental covariance is given by the matrix:

$$[CR_{jk}] = [\hat{n}(r_j)\hat{n}(r_k) - 1] \tag{5.8}$$

Assuming the angular separation of the binary source is small then the expected values of these matrix elements are a function only of the separation between detector elements. Therefore, elements along diagonals parallel to the main diagonal are expected to be equal in the absence of noise. Using this fact, the spatioangular covariance of counts as a function of detector element separation is formed by summing along these diagonals as indicated here.

$$[CR_{jk}] \rightarrow [CR_k] \text{ by } \begin{bmatrix} \hat{n}(r_1)\hat{n}(r_1) & \hat{n}(r_1)\hat{n}(r_2) \ldots & \hat{n}(r_1)\hat{n}(r_{10}) \\ \hat{n}(r_2)\hat{n}(r_1) & \hat{n}(r_2)^2 & \\ \hat{n}(r_3)\hat{n}(r_1) & \hat{n}(r_3)\hat{n}(r_2) & \\ \vdots & & \\ \hat{n}(r_{10})\hat{n}(r_1) & & \hat{n}(r_{10})\hat{n}(r_{10}) \end{bmatrix} \tag{5.9}$$

Since the number of terms along these diagonals are not equal, then the elements of this sum must be normalized by the number of terms to preserve the relationship of equation 5.4. Therefore, the elements of the measured covariance vector are written:

$$CR_k = \left(2(10-|n-m|)\right)^{-1} \sum_{\substack{n=1,10-k \\ m=n+k}} \left[CR_{nm} + CR_{mn}\right] \qquad (5.10)$$

and, the structure parameter profile is determined by solving the matrix equation

$$\left[\sum_k \left(R_{k,i}\, R_{k,j}\right)\right] \left[C_n^2(h_j)\right] = \left[\sum_k \left(R_{k,j}\, CR_k\right)\right] \qquad (5.11)$$

Which results from applying least squares analysis with the parameters $C_n^2(h_j)$ the undetermined coefficients. The profile is now determined since the detector element separation and altitude are connected by the relation 3.1.

VI. CONCLUSIONS

This thesis has explored the theoretical basis for profiling the refractive index structure parameter using the spatial covariance of binary source intensity scintillations. This analysis derived the power spectrum and associated spatial covariance of intensity scintillations caused by atmospheric refractive turbulence. The expected spatial covariance of photoelectron (photon) counts and counting statistics were derived using the intensity covariance functions.

No rigorous analysis of the binary source technique as implemented by several French teams [Refs. 12-15] is currently available in the open literature; and, the analysis of this thesis reveals several interesting features not previously noted.

The power spectrum and spatial covariance used by the French teams are essentially correct; however, the error analysis of the binary source technique is incomplete. A consideration of the photoelectron counting statistics indicates that very large relative errors of 200 to 2,000 percent are expected in any determination of the spatial covariance function. This large error is not significantly improved by increasing the counting rate above unity as indicated by Figure 8. Previous experimental work [Refs. 12-15] was limited to bright (magnitude 2) stellar binaries. However, an elementary calculation of the available photons per counting time (approximately one msec) coupled with the relative insensitivity of the binary source technique to increased counting rates indicates that stellar

binaries of magnitudes three to four are also suitable for detector apertures of 30 to 60 centimeters.

The large relative error expected in an experimental determination of the spatial covariance necessitates the use of a smoothing algorithm and the least squares technique was selected. The advantage of least squares analysis is that it accomplishes the two-fold purpose of data smoothing and refractive index structure parameter profiling. The basis selected for the least squares analysis is the nonorthogonal set of theoretically derived spatial covariance functions for a series of atmospheric layers of increasing attitude. The weighting coefficients derived using the least squares algorithm are found to be the required refractive index structure parameters for the atmospheric layers.

The expected improvement in the relative error remains an open-ended question. The error analysis depends on the intermittency of atmospheric turbulence and as indicated in Section IV, the error analysis in this thesis constitutes a lower bound for the expected error. Clearly, further work on the intermittent aspects of atmospheric turbulence is indicated.

Despite the large errors expected in the determination of the spatial covariance function the binary source technique has several clear advantages. As mentioned in the Introduction, the altitude resolution of the binary source technique is superior to that of existing methods. The implementation of the least squares algorithm is straightforward and results in a relatively unambiguous determination of the structure parameter profile. Modest aperture sizes (30 to 60 cm) are adequate for the detector system. The greatest disadvantage of the technique is the paucity

of suitable stellar binaries. However, by using stellar sources of up to magnitude four this drawback becomes minor.

Based on this analysis, experimental implementation of this technique should proceed, and the experimental profiles obtained should be compared with insitu measurements or integrated profiles such as that produced by stellar scintillometers [Ref. 16].

REFERENCES

1. Gossard, E.E., Gaynor, J.E., Zamora, R.J., and Neff, W.D., "Fine-structure of Elevated Stable Layers Observed by Sounder and In Situ Tower Sensors," Journal of the Atmospheric Sciences 42, pp. 2156-2159, 1985.

2. Little, C.G., "Acoustic Methods for Remote Probing of the Lower Atmosphere," Proceedings of the IEEE 57, pp. 571-578, 1969.

3. Gage, K.S., Green, J.L., and Van Zandt, "Use of Doppler Radar for the Measurement of Atmospheric Turbulence Parameters from Intensity of Clear-Air Echoes," Radio Science 15, pp. 407-416, 1980.

4. Bean, B.R., "Applications of FM-CW Radar and Acoustic Echosounder Techniques to Boundary Layer and CAT Studies," Remote Sensing of the Troposphere, Chapter 20, U.S. Government Printing Office, Washington, D.C., 1972.

5. Bufton, J.L., Menoh, T.T., Fitzmaurice, N.W., "Measurement of Turbulence Profiles in the Troposphere," Journal of the Optical Society of America 62, pp. 1068-1070, 1972.

6. Heneghan, J.M., and Ishimaru, A., "Remote Determination of the Profiles of the Atmospheric Structure Constant and Wind Velocity Along a Line-of-Sight Path by a Statistical Inversion Procedure," IEEE Transactions on Antennas and Propagation AP-22, pp. 457-464, 1974.

7. Peskoff, A., "Theory of Remote Sensing of Clear-Air Turbulence Profiles," Journal of the Optical Society of America 58, pp. 1032-1040, 1968.

8. Lee, R.W., "Remote Probing Using Spatially Filtered Apertures," Journal of the Optical Society of America 64, pp. 1295-1300, 1974.

9. Clifford, S.F., and Churnside, J.H., "Refractive Turbulence Profiling Using Synthetic Aperture Filtering of Scintillation," Applied Optics 26, pp. 1295-1303, 1987.

10. Fisher, M.J., and Krause, F.R., "The Crossed-Beam Correlation Technique," Journal of Fluid Mechanics 28, pp. 705-717, 1967.

11. Wang, T., Clifford, S.F., and Ochs, G.R., "Wind and Refractive-Turbulence Sensing Using Crossed Laser Beams," Applied Optics 13, pp. 2602-2608, 1974.

12. Rocca, A., Roddier, F., and Vernin, J., "Detection of Atmospheric Turbulent Layers by Spaciotemporal and Spacioangular Correlation Measurements of Stellar-Light Scintillation," Journal of the Optical Society of America 64, pp. 1000-1004, 1974.

13. Roddier, C., and Vernin, J., "Relative Contribution of Upper and Lower Atmosphere to Integrated Refractive-Index Profiles," Applied Optics 16, pp. 2252-2256, 1977.

14. Azouit, M., and Vernin, J., "Remote Investigation of Tropospheric Turbulence by Two-Dimensional Analysis of Stellar Scintillation," Journal of the Optical Society of America 37, pp. 1550-1557, 1980.

15. Azouit, M., Vernin, J., Barletti, R., Ceppatelli, G., Righini, A., and Speroni, N., "Remote Sensing of Atmospheric Turbulence by Means of a Fast Optical Method: A Comparison with Simultaneous In Situ Measurements," Journal of Applied Meteorology 19, pp. 834-838, 1980.

16. Stevens, K.B., Remote Measurement of the Atmospheric Isoplanatic Angle and Determination of Refractive Turbulence Profiles by Direct Inversion of the Scintillation Amplitude Covariance Function with Tikhonov Regularization, Doctoral Dissertation, Naval Postgraduate School, Monterey, California, December, 1985.

17. Walters, D.A., Private Communication, June 15, 1988, Naval Postgraduate School, Monterey, California.

18. Tatarski, V.I., Wave Propagation in a Turbulent Medium, Dover Publications, New York, p. 1967, 1961.

19. Clifford, S.F., "The Classical Theory of Wave Propagation in a Turbulent Medium," Topics in Applied Physics, Laser Beam Propagation in the Atmosphere, Vol. 25, Chapter 2, Springer-Verlag, New York, 1978.

20. Tennekes, H. and Lumely, J.L., A First Course in Turbulence, The M.I.T. Press, Cambridge, Massachusetts, 1972.

21. Batchelor, G.K., The Theory of Homogeneous Turbulence, Cambridge University Press, London, U.K., 1953.

22. Hanbury-Brown, R., and Twiss, R.Q., "A Stellar Interferometer Based on the Principle of Intensity Interferometry," Interferometry, London: Her Majesty's Stationary Office, 1960.

23. Fried, D.L., "Aperture Averaging of Scintillation," Journal of the Optical Society of America 57, pp. 169-174, 1967.

24. Kleen, R.H., and Ochs, G.R., "Measurement of Wavelength Dependence of Scintillation in Strong Turbulence," Journal of the Optical Society of America 60, pp. 1695-1697, 1970.

25. Saleh, B., Springer Series on Optical Sciences Photoelectron Counting Statistics, Springer-Verlag, New York, 1978.

26. Papoulis, A., Probability, Random Variables, and Stochastic Processes, McGraw Hill International, New York, 1984.

INITIAL DISTRIBUTION LIST

		No. Copies
1.	Defense Technical Information Center Cameron Station Alexandria, Virginia 22304-6145	2
2.	Library, Code 0142 Naval Postgraduate School Monterey, California 93943-5002	2
3.	Donald L. Walters Code 61 We Naval Postgraduate School Monterey, California 93943-5004	10
4.	E. Rockower Code 55 RF Naval Postgraduate School Monterey, California 93943-5000	2
5.	K. E. Woehler Code 61 Chairman, Physics Department Naval Postgraduate School Monterey, California 93943-5000	2
6.	Lt. R. R. Holland, USNR 2495 11th Court SW Vero Beach Highlands Vero Beach, Florida 32962	2